



HAL
open science

Bedload tracing with RFID tags in gravel-bed rivers: Review and meta-analysis after 20 years of field and laboratory experiments

Frédéric Liébault, Hervé Piégay, Mathieu Cassel, Fanny Arnaud

► **To cite this version:**

Frédéric Liébault, Hervé Piégay, Mathieu Cassel, Fanny Arnaud. Bedload tracing with RFID tags in gravel-bed rivers: Review and meta-analysis after 20 years of field and laboratory experiments. *Earth Surface Processes and Landforms*, 2023, pp.1-23. 10.1002/esp.5704 . hal-04205726

HAL Id: hal-04205726

<https://hal.science/hal-04205726>

Submitted on 13 Sep 2023

HAL is a multi-disciplinary open access archive for the deposit and dissemination of scientific research documents, whether they are published or not. The documents may come from teaching and research institutions in France or abroad, or from public or private research centers.

L'archive ouverte pluridisciplinaire **HAL**, est destinée au dépôt et à la diffusion de documents scientifiques de niveau recherche, publiés ou non, émanant des établissements d'enseignement et de recherche français ou étrangers, des laboratoires publics ou privés.



Distributed under a Creative Commons Attribution - NonCommercial - NoDerivatives 4.0 International License

Bedload tracing with RFID tags in gravel-bed rivers: Review and meta-analysis after 20 years of field and laboratory experiments

Frédéric Liébault¹  | Hervé Piégay²  | Mathieu Cassel²  | Fanny Arnaud² 

¹Université Grenoble Alpes, INRAE, CNRS, IRD, Grenoble INP, IGE, Grenoble, France

²Université de Lyon, EVS, CNRS-UMR 5600, ENS, Lyon, France

Correspondence

Frédéric Liébault, INRAE, Domaine Universitaire, 2 rue de la Papeterie BP76, Saint-Martin-d'Hères 38402, France.
Email: frederic.liebault@inrae.fr

Abstract

Soon after their first deployment in rivers in the early 2000s, RFID tags rapidly became the reference technology for bedload tracing in rivers. We can estimate from the literature that during the last 20 years, more than 30,000 RFID tracers have been injected in gravel-bed rivers all around the world to study bedload transport. Many field experiments have been reported in a great diversity of fluvial environments, complemented by many laboratory experiments and methodological developments. This paper proposes a review of these works, notably based on the compilation of more than 350 RFID surveys, complemented by 97 magnetic surveys, for a total of 125 study sites. The meta-analysis of this database shows that RFID tracers have improved our understanding of sediment transport in fluvial environments with rapid bedload dispersion. It is also shown that central positions of tracer plumes are moving faster over time than tracer leading fronts, as attested by a general relation between maximum and mean distances of transport. The most recent methodological developments based on the use of active UHF RFID tags show that it is now possible to conduct efficient bedload tracing experiments not only in small streams, but also in large gravel-bed rivers or very active braided channels. Other addressed topics include RFID deployment and survey in river channels, controlling factors of tracer mobility (flow conditions, grain-size and shape, channel morphology), bedload monitoring approaches using RFID tracers, and applications of RFID tracers for evaluating human effects on bedload transport. Key challenges of bedload tracing with RFID tags are also proposed.

KEYWORDS

bedload dispersion, bedload transport, gravel-bed rivers, RFID tracing, sediment management

1 | INTRODUCTION

Sediment tracing is a long-standing approach for the study of bedload transport in gravel-bed rivers. The idea of tracking the displacement of individual particles constituting the bed material of river channels (referred to here as bedload dispersion) appeared in the 1930s, with the random walk vision of bedload transport initiated by Hans Albert Einstein in 1937. One of the main interests of this approach is the possibility to determine the bedload flux from physical variables

describing random tracer motion. Different formalisms of this stochastic approach of bedload transport integrate many variables that can be more or less consistently measured with tracers, such as the entrainment rate of bed particles, the travel distance, the virtual velocity, the step length or the resting time of mobile tracers (see Hassan & Bradley, 2017, and Mao et al., 2020, for reviews of bedload flux computations using tracers). Tracers have also been of great help for addressing many fluvial processes related to the transport of individual coarse particles, such as downstream fining, propagation of

This is an open access article under the terms of the [Creative Commons Attribution-NonCommercial-NoDerivs](https://creativecommons.org/licenses/by-nc-nd/4.0/) License, which permits use and distribution in any medium, provided the original work is properly cited, the use is non-commercial and no modifications or adaptations are made.

© 2023 The Authors. *Earth Surface Processes and Landforms* published by John Wiley & Sons Ltd.

sediment waves or interactions between bedload transport and channel morphology.

Since the second international Gravel-Bed Rivers (GBR) Workshop in 1985, the topic of bedload tracing has been regularly covered in GBR book chapters and proceedings, providing successive scientific reports on technological advances and associated research findings on this topic (Ferguson et al., 1998; Hassan & Bradley, 2017; Hassan & Church, 1992; McEwan et al., 2001; Schick et al., 1987). The last review by Hassan and Bradley (2017) pointed out the emergence and increasing use of radio frequency identification (RFID) for bedload tracing, but the authors concluded that *our understanding of grain-scale bedload motion in river channels is still limited by our technological capacity for the real-time tracking of grain displacement in a wide range of natural conditions*. RFID developments since this last review open the opportunity to fill this gap.

The first field experiments with passive RFID tags in river channels date back to the early 2000s. They showed high recovery rates (>80%) for populations of deployed tracers >100 in a semi-arid sand-bed stream in Arizona (Nichols, 2004) and a small boulder-bed stream in Quebec (Lamarre et al., 2005). Soon after these early promising results, passive RFID rapidly became the reference technology for bedload tracing in rivers. From the early 2000s, they progressively replaced the most commonly used tracing techniques, such as painted or magnetic stones (Hassan & Ergenzinger, 2003). We can estimate from the literature that during the last 20 years, more than 30 000 RFID tracers have been injected in rivers all around the world. This recent popularity of passive RFID tags in coarse sediment tracing is based on several decisive advantages; they provide low-cost (<5 €), long-lived (>10 years) and small-size (<35 mm) tracers that can be remotely detected and identified, even when buried under a sediment layer of several decimetres. Although buried magnetic stones can also be detected with recovery rates comparable to RFID tags, their identification is only possible after time-consuming and intrusive excavations of alluvial deposits, whose structural properties became disturbed. The only alternative solution for remote identification of

tracer stones is battery-powered very high frequency (VHF) radio transmitters that have been used since the late 1980s (e.g., Chacho et al., 1989; Ergenzinger et al., 1989; Schmidt & Ergenzinger, 1992), but their high cost and short lived have limited their field employment to very small populations of active tracers (generally less than 30) monitored during very short periods (typically one hydrological season). Unlike passive RFID tags, radio transmitters can be detected at long distances (up to 800 m), which is a great advantage for field surveys, notably in large gravel-bed rivers. However, several recent field experiments have shown that the application domain of RFID tags can be strongly increased with active ultra-high frequency (UHF) RFID tags (Brousse, Arnaud-Fassetta, et al., 2020; Cassel, Dépret, et al., 2017), which are much more affordable than VHF radio transmitters.

When looking at the bedload tracing scientific production of the last 20 years, it becomes clear that a disruptive technological step occurred with the diffusion of RFID in bedload transport research, with 70 published papers in peer-review scientific journals between 2004 and 2021 (Figure 1) and more than 400 reported field surveys in a great diversity of fluvial environments. These range from small boulder-bed streams (<5 m in channel width, w) to large gravel-bed rivers ($w > 200$ m) and from semi-arid to temperate and tropical climatic settings, including all types of hydrological regimes (intermittent, pluvial, Mediterranean, snowmelt and glacial-melt). Several flume experiments using RFID tags have also been reported. The thematic field covered by this corpus is very rich (Figure 1), with many contributions on physical mechanisms and properties of bedload transport (referred to here as 'physical studies', $n = 35$), on the monitoring of river management and restoration works ('management applications', $n = 22$) and on methodological works using experimental facilities and/or field tests ('methodological advances', $n = 13$).

Based on this corpus of published papers and additional conference proceedings and academic reports presenting results from RFID tracers, a database of 362 RFID surveys and 97 magnetic surveys was compiled, for a total of 125 study sites (see the [supporting](#)

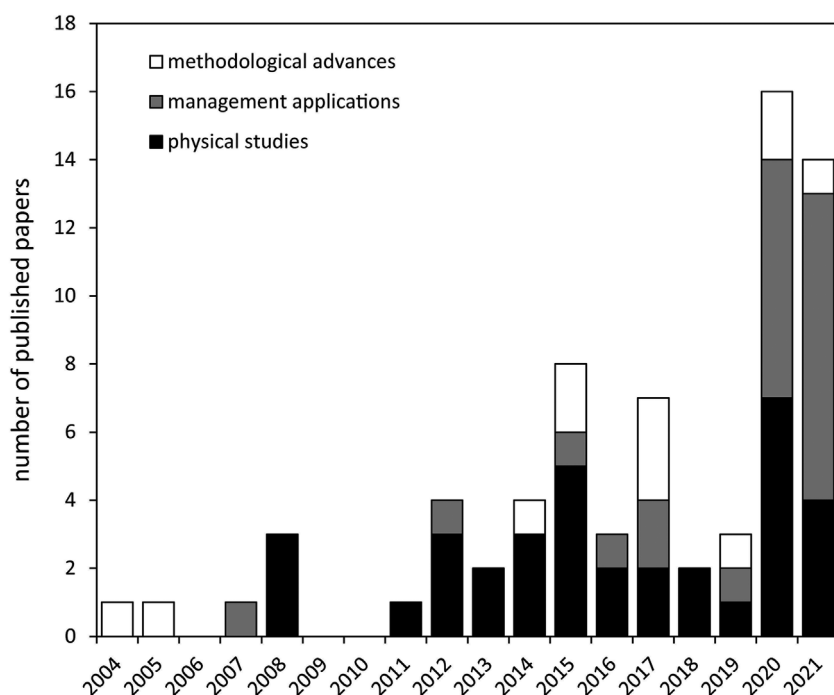


FIGURE 1 Time evolution of the number of scientific publications reporting RFID applications in fluvial bedload tracing between 2004 and 2021. Only papers published in peer-review scientific journals were considered. Selection of papers was based on an ad hoc procedure combining the Scopus database and citations from selected papers. Papers were classified in three groups (methodological advances, physical studies and management applications) according to the primary objective of the study (see Tables S1 and S3).

information for details about the corpus inventory and data compilation). This database was used to provide a comprehensive and synthetic meta-analysis of RFID studies of the last 20 years, by addressing successively (i) how RFID tags have been deployed and surveyed in river channels and what have been the main achieved methodological advances, (ii) what has been the contribution of RFID tags to the observation and understanding of bedload transfer in gravel-bed channels, (iii) how RFID tags have been used for the monitoring of river management and restoration works and (iv) what are the key challenges of RFID bedload tracing for the next years.

2 | RFID DEPLOYMENT AND SURVEY IN RIVER CHANNELS

2.1 | General assumptions of the bedload tracing approach

Tracking the displacement of individual particles for the study of bedload is based on the overarching assumption that tracers are representative of mobile bed particles that constitute bedload transport during a given hydrological period. Tracers can then be surveyed to obtain the most widely used random variables of bedload transport such as the distance of transport (total displacement length during the survey period, which is the sum of individual step lengths) or the virtual velocity (average tracer velocity over the transporting event, including periods of rest and motion; the virtual velocity is thus lower than the 'true' velocity of tracers during motion periods). To be representative, bedload tracers should well reproduce physical properties of bedload particles (size, shape and density). Their seeding in river channels should consider the spatial heterogeneity of alluvial landforms, which are typically organized in assemblages of elementary morphological units (e.g., riffle, pool and bar). The vertical sediment sorting (surface and subsurface layers) as well as sedimentary structures of river beds (e.g., imbrication and clustering) should be considered too. The recovery rate of mobile tracers should be as high as possible to make sure that a specific sub-population of tracer has not been under-represented in the spreading plume of tracers (e.g., frontrunners and deeply buried tracers). Finally, considerations of sample size have also direct implications for the statistical representativeness of the true population (all the individual particles contributing to bedload transport of a given study reach during a given time period). These requirements can vary depending on the main objective of the tracing experiment (e.g., bedload transport estimation from travel distance or virtual velocity, fitting stochastic parameters in dispersion models, estimating critical shear stress, describing vertical mixing, selective transport and interactions between bedload transport and channel morphology), but this point is beyond the scope of this paper. With those general assumptions in mind, advantages and limitations of RFID solutions for bedload tracing are presented in the following sub-sections.

2.2 | RFID tags, tracer stones and antennas

RFID can be defined as a set of technologies for wireless detection and identification of objects based on a radiofrequency

communication channel. Two types of RFID systems exist: (i) passive RFID based on a transponder without battery that is powered by the electromagnetic wave produced by a reader and that backscatters a modulated signal containing identification information and (ii) active RFID based on an electronic device with an on-board battery that periodically emits its own radiofrequency wave with a unique identification code to a reader (see Le Breton et al., 2022, for technological basics of RFID). The great advantage of passive RFID as compared to radio transmitters traditionally used in animal or sediment radio-tracking telemetry is that the backscattering energy is delivered by the detection antenna and not by an internal battery with its limited lifespan (generally less than 2 years for radio transmitters). Active RFID shares some similarities with radio transmitters, since a battery is used for emission of the radiofrequency wave, but these two active radio-tracking solutions have their own pros and cons with respect to bedload tracing (see below).

Several types of passive RFID tags have been employed for bedload tracing, with different technical specifications, shapes and sizes (Table 1). The most commonly used are glass-encapsulated needle-shape tags of 23- or 32-mm length (called PIT tags, for Passive Integrated Transponders). Smaller 12-mm tags have also been used (Cain & McVicar, 2020; Imhoff & Wilcox, 2016; Magilligan et al., 2021; McQueen et al., 2021; Papangelakis, Muirhead, et al., 2019), but their very short detection range (around 0.20 m according to Chapuis et al., 2014) has limited their field deployment. Passive tags have been very attractive for bedload applications because their low cost offers the possibility to deploy very large populations of tracers. Several campaigns including more than 1000 tracers per seeding site have been implemented (Arnaud et al., 2017; Chardon et al., 2021; Dépret, 2014; Olinde & Johnson, 2015). However, these tags can only be detected at a short distance, typically less than 1 m, and time-consuming field surveys with mobile antennas are needed when tracers have been displaced along channel reaches over length scales of kilometres (e.g., Arnaud et al., 2017; Liébault et al., 2012; Olinde & Johnson, 2015). Another disadvantage of low-frequency tags is related to signal collision, preventing the simultaneous detection of tags close to each other (tracer clustering). Some anti-collision techniques exist (Lauth & Papanicolaou, 2009; Tsakiris et al., 2015), but they are not commonly used. These two technical drawbacks have been presented as factors explaining low recovery rates, notably in large rivers (see Section 2.3). Their optimal application domains are therefore small streams with low bedload mobility, and alternative RFID solutions have been explored for large rivers or fluvial environments with high bedload mobility.

Several recent tests were done with active UHF (433.92 MHz) RFID tags offering interesting technical performances due to their anti-collision protocol and battery-powered UHF signal. They thus offer a much higher detection range than PIT tags (from 80 to 150 m in the air, according to manufacturers), but at the expense of a higher unit cost (around 45 € per tag, and 70 € per artificial tracer stone, this price including the manufacturing cost of the artificial stone), a much larger volumetric size (Table 1) and a shorter life span. This latter is around 10 years, but it depends on the time interval of signal emission, which can be parameterized for each tag. Although active tags have a lower longevity than PIT tags, their life span is not a strong limiting factor for most bedload tracing experiments, these rarely exceeding 5 years. Like radio transmitters, active RFID tags emit their own

TABLE 1 Technical specifications and dimensions of RFID tags used for bedload tracing.

Tag reference	Type of tag/frequency	Shape, dimensions and volume	Maximum detection range (m)
12-mm PIT tag ^a	Passive/LF 134.2 kHz	Cylindrical (needle shape), 2.15 mm diameter, 12 mm length, 44 mm ³	0.20
23-mm PIT tag ^a	Passive/LF 134.2 kHz	Cylindrical (needle shape), 3.65–3.85 mm diameter, 23 mm length, 268 mm ³	0.72
32-mm PIT tag ^a	Passive/LF 134.2 kHz	Cylindrical (needle shape), 3.65–3.85 mm diameter, 32 mm length, 373 mm ³	0.95
M100 ^b	Active/UHF 433.92 MHz	Rectangular, 56.4 × 46.6 × 11.2 mm, 18 714 mm ³	91
COIN-HC ^c	Active/UHF 433.92 MHz	Cylindrical (coin shape), 40 mm diameter, 15 mm length, 18 850 mm ³	80
COIN-ID ^c	Active/UHF 433.92 MHz	Cylindrical (coin shape), 36 mm diameter, 11.5 mm length, 11 706 mm ³	80
PUCK-ID ^c	Active/UHF 433.92 MHz	Cylindrical (coin shape), 57 mm diameter, 20 mm length, 51 035 mm ³	150

Note: The maximum detection ranges are from Chapuis et al. (2014) for 12-mm PIT tags, Arnaud et al. (2015) for 23 and 32-mm PIT tags and from manufacturer's documentations for active tags. Detection ranges are considered in the atmospheric medium. The effect of water on detection ranges is negligible for passive tags (less than 10% decrease according to Arnaud et al., 2015) but much stronger for active tags (maximum detection range of 2.4 m in water for COIN-HC, according to Cassel, Dépret, et al., 2017).

^aFrom TIRIS Technology or HDX Oregon RFID.

^bFrom RF Code Inc.

^cFrom ELA innovation SA.

radiofrequency wave at a regular interval but operate in the UHF frequency band (vs VHF band for radio-transmitters). This implies a stronger signal attenuation in water for active RFID, as compared to radio transmitters. Radio transmitters thus offer better performance in detection ranges, with commonly reported values of several hundred metres (Habersack, 2001; Liedermann et al., 2013; May & Pryor, 2014), and the most sophisticated ones incorporate a motion sensor, delivering information about step lengths and rest periods (Habersack, 2001; May & Pryor, 2014; McNamara et al., 2008; McNamara & Borden, 2004). However, active UHF RFID tags offer a much more affordable tracking solution than radio transmitters (i.e., 350€ per stone equipped with a VHF radio transmitter in Klösch & Habersack, 2018, this price including the manufacturing cost of artificial stone). Although it is now possible to assign a unique ID to radio transmitters, allowing multiple different tags to be detected on a single VHF frequency, with the possibility to track thousands of tags if several frequencies are used, the unit cost of these tags remains far too high to envisage the deployment of large populations of tracers. Moreover, the lack of anti-collision protocol for radio transmitters can lead to detection problems related to tracer clustering.

The first reported test with active RFID tags (40-mm diameter COIN-HC) showed maximum detection ranges of 2.4 and 2.6 m in water and in water-saturated sediment, respectively, as well as the possibility to use the *RSSI* (Received Signal Strength Indication) for determining the tag position with an accuracy of <1 m (Cassel, Dépret, et al., 2017). Three other active UHF tags have been used to date for bedload tracing: M100 already used for the tracking of floating wood pieces (McVicar et al., 2009), COIN-ID with exactly the same electronic chips as the COIN-HC but with a more compact design and PUCK-ID, a bigger tag with a higher detection range (Cassel et al., 2020; Cassel, Piégay, et al., 2017). Due to the coin-like shape of active tags, their inlay in natural stones is less easy, and they are generally cast into synthetic stones made with a mixture of polyurethane resin and corundum to be able to get a density equivalent to natural

stones (Brousse, Arnaud-Fassetta, et al., 2020; Cassel et al., 2020). Laboratory experiments in an annular flume with synthetic stones equipped with active tags showed that COIN-ID were more resistant to shock during transport than M100 (Cassel, Piégay, et al., 2017).

RFID tags are generally inserted into particles by drilling or notching natural stones sampled in the field. For the smaller grain sizes that easily fracture while being drilled, it has been proposed to use artificial stones built with synthetic resin or concrete (e.g., Olinde & Johnson, 2015; Schneider et al., 2014). The range of investigated grain-sizes is constrained by the size of the transponder, and the smallest tracers are generally comprised between 20 and 40 mm in *b*-axis. The upper end of tracer size is not limited, but it is generally fixed according to the coarse tail of the local bedload or bed-material grain-size distribution (GSD). Some field experiments have used a narrow GSD of tracers aligned with the channel D_{50} to minimize variability in transport characteristics (Bradley & Tucker, 2012; Phillips & Jerolmack, 2014), but wide ranges of tracer sizes can be also employed for matching as much as possible the bed-material GSD or for addressing size-selective transport (see Table S1).

Once equipped with tags, RFID tracer stones are measured and deployed in river channels, and their displacement after a period with one or multiple transporting flow events is surveyed by manual detection and mapping of displaced tracers using a mobile antenna and a positioning system (e.g., dGPS and total station). Standard operating procedures for PIT tag detection using mobile antennas have been proposed (Arnaud et al., 2015; Chapuis et al., 2014). These are based on analysis of the effects of tag orientation and size on 3D detection envelopes for different antenna configurations and sizes, as well as experimental tests dedicated to the effect of the surrounding medium (water, dry sediment and water-saturated sediment) on detection ranges. Although contrasted results have been reported, it can be generally considered that the effect of the surrounding medium on PIT tag detection range is low, with a typically less than 10% reduction in water or water-saturated sediment as compared to open-air

conditions (Arnaud et al., 2015). However, it has been shown that tag orientation has a strong effect on 3D detection envelopes, with best conditions of detection when the tag is perpendicular to the antenna loop (Arnaud et al., 2015; Chapuis et al., 2014). It has been therefore recommended to insert transponders along the *c*-axis of stones to maximize the chance of detection. These methodological works also show that due to contrasting detection envelopes associated with different antenna configurations and sizes, it could be interesting to combine different antenna designs during field surveys, notably when a strong clustering of RFID tracers is suspected (McQueen et al., 2021).

Another field strategy is to use a stationary antenna along a cross-section to automatically detect RFID tracers passing through the monitoring section. This has not been widely used so far, mainly because short reading distances of passive low-frequency tags require fixing antennas at the river bed, and these can be disturbed or damaged during floods (Stähly et al., 2020). Another reason is the higher cost of those antennas as compared to mobile ones. Despite these technical difficulties, it has been shown that four stationary antennas spaced 50-m apart can be successfully used to constrain the virtual velocity of tracers in a 6-m wide proglacial boulder-bed stream, where the daily melting flow regime during summer hinders channel survey with a portable antenna (Mao, Dell'Agnese, et al., 2017). This RFID monitoring strategy has been used for the first time in a 4-m wide glacier-fed step-pool stream in Switzerland, showing a 39% maximum detection rate of passing tracers (Schneider et al., 2010). More recently, a stationary antenna has been deployed in a 25-m wide gravel-bed river to monitor the virtual velocity of tracers seeded in artificial gravel deposits, showing a detection rate less or equal to 16% (Stähly et al., 2020). Similar results were obtained with an antenna fixed along a 5.4-m wide low-head dam in a small gravel-bed stream in Ireland, with a detection rate of 18% (Casserly et al., 2021). A much higher detection rate of 100% was recently obtained with a stationary antenna specifically designed for the detection of active UHF RFID tags (Cassel, Navratil, et al., 2021). This non-intrusive prototype is adapted to harsh outdoor environments. It allowed capturing the velocity of tracers equipped with COIN-ID along a 60-m long reach of a 12-m wide gravel-bed river in the French Alps.

2.3 | Design of bedload tracing experiments

A variety of bedload tracing designs have been proposed to achieve the best compromise between study objectives, experiment duration, fluvial environment, and available financial and human resources. The number of deployed tracers strongly depends on the tracer unit cost, mainly determined by the RFID tag cost. Tracer populations per seeding site are ranging from ~25 to ~1500 tracers for low-cost passive tags and from ~30 to ~150 tracers for high-cost active tags. Although experiments reported for large rivers are always based on large populations of tracers (>1000; see Section 2.4), we did not find any systematic increase of the tracer sample size with the size of the river. This shows that the sample size is mainly determined by available financial and human resources for tracer equipment and preparation.

The spatio-temporal design of tracer seeding can involve one or several seeding sites that can be repeated over time. Single-site

designs are referred to here as field experiments for which tracers are considered as representative of a single river reach, even if tracers may have been injected in different morphological units of the active channel (e.g., gravel bars, pools and riffles). It is the most-commonly used design of RFID tracer studies. Multi-site designs are employed when emphasis is placed on comparing tracer mobility in different fluvial conditions, either different reaches of the same river or different rivers. The former is well adapted for assessing the influence of a variety of factors on bedload mobility, like sedimentary structures (Lamarre & Roy, 2008a), morphological gradients (Chardon et al., 2021; McQueen et al., 2021; Rollet, 2007), glacial imprint (Dell'Agnese et al., 2015) or artificial features like dams or weirs (Casserly et al., 2020; Magilligan et al., 2021; Peeters et al., 2020; Roberts et al., 2020). Tracing experiments involving several rivers have been focused on assessing the effects of hydrology (Gilet et al., 2020; Houbrechts et al., 2015; Phillips & Jerolmack, 2014), tributary confluences (Imhoff & Wilcox, 2016), stream restoration (Papangelakis & MacVicar, 2020) and human pressures (Galia et al., 2021; Papangelakis, McVicar et al., 2019). In the case of repeated tracer deployments, the main purpose is to maintain a high number of tracers through time for event-based surveys from which scaling laws can be obtained between bedload mobility and hydrological predictors (e.g. Brenna et al., 2019; Dell'Agnese et al., 2015; Gilet et al., 2020; Mao et al., 2020; McQueen et al., 2021; Oss Cazzador et al., 2021; Schneider et al., 2014). Repeated seeding can also be useful when one or several stationary antennas are used, to ensure a high number of detections through time (Mao, Dell'Agnese, et al., 2017).

At the site scale, different modes of tracer deployment have been employed. These are not radically different from those adopted with magnetic stones. The cluster mode (several tracers deployed simultaneously at a single point) is a recourse for the seeding of numerous tracers in high flow velocity and/or deep-water zones (Misset et al., 2020) or in the volume of a replenished sediment (Stähly et al., 2020). This mode is not widely used because of signal collision effects preventing the detection of immobile tracers when PIT tags are used. The grid (Bradley & Tucker, 2012) and cross-section (Lamarre et al., 2005) modes, which consist in deploying tracers individually at regular intervals along a grid or a cross-section, are usually preferred to avoid signal collision. Another advantage of these approaches is the possibility to seed different morphological units of the channel and to compare their contribution to bedload transport (Liébault et al., 2012; McQueen et al., 2021). Whatever the deployment mode, tracers are generally deposited at the surface of the alluvial bed, without being embedded in the sedimentary structure, contrary to painted tracers that can be spray-painted in place. This may lead to an artificial mobility during the first survey after deployment. Even if different field strategies have been used to reduce this artefact (Hassan & Roy, 2016), some authors exclude displacement data from the first mobilizing flow event after tracer deployment (e.g., Houbrechts et al., 2012; Lamarre & Roy, 2008b).

In dry or wadable channels at low flow, field surveys with a mobile antenna are conducted by human operators carrying the RFID reading system (Figure 2a,b). Spacing between walked survey lines depends on the antenna detection range and is typically of 1 to 2 m and up to 10–20 m, for PIT tags and for active UHF tags, respectively. In non-wadable channels, the RFID equipment is shipped on a boat (Figure 2c). The antenna is towed and should be maintained as close

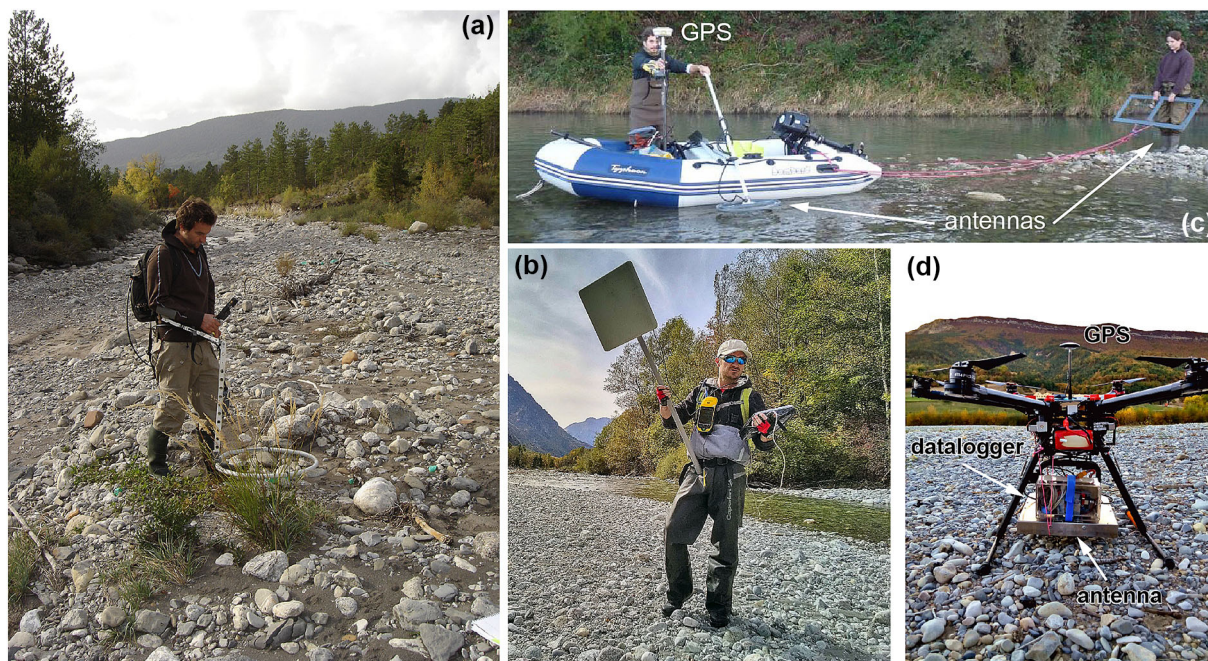


FIGURE 2 Methods for RFID surveys in river channels using a mobile antenna in wadable zones for passive (a) and active (b) RFID tracers, a boat in a non-wadable large aquatic channel (c) and a UAV equipped with a RFID antenna and a GPS for the survey of active UHF tags in a large braided gravel-bed river (d).

as possible to the channel bottom (Arnaud et al., 2017). The spacing between passages should remain <3 m for both PIT tags and active UHF tags, which is not easy to conduct in large channels and/or rapid flows. When the water depth exceeds 3 m, a more secured tracking solution is battery-powered radio transmitters (Klösch & Habersack, 2018; Liedermann et al., 2013). Active UHF tags can also be detected in shallow channels and emerged areas using Unmanned Aerial Vehicles (UAVs) (Figure 2d). Accuracy in tracer positioning and speed of survey have been characterized in a braided river reach with a UAV flying at a height of 8 m above the ground, at a flight speed of 1.5 m s^{-1} and following a grid plan with 10-m spaced passages (Cassel et al., 2020). Using this method, 84% of the tracers were detected with a better than 5-m mean accuracy in tracer positioning. Thus, the UAV solution is particularly suitable for large and poorly vegetated gravel-bed channels, and for ground surfaces with a rough topography. Airborne RFID surveys require synchronization of the RFID antenna with the GPS through an integrated platform of detection and positioning. This can be also very useful when surveying by boat to reduce the number of operators.

2.4 | Recovery rates

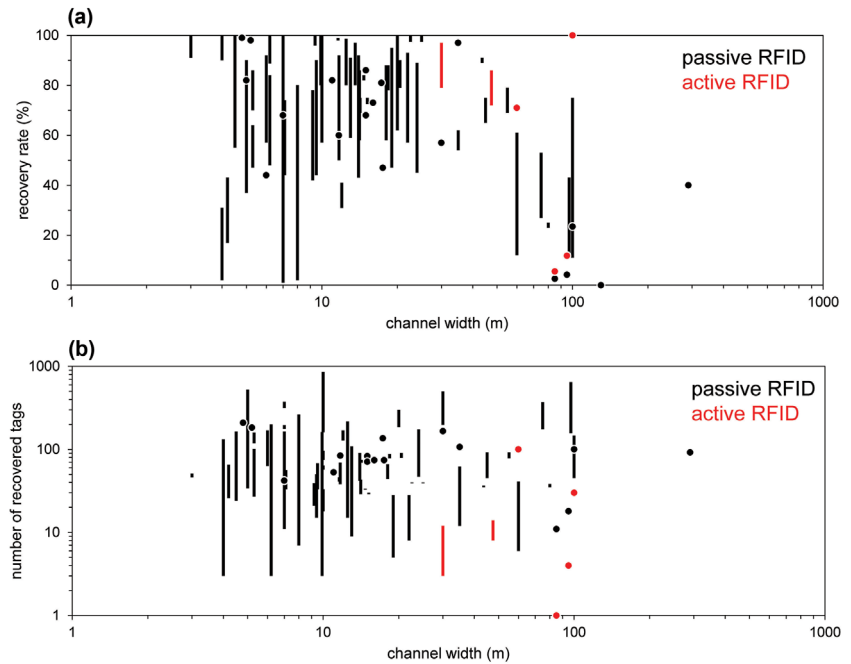
The quality of data from tracing experiments is commonly evaluated with the recovery rate, which can be calculated based on all recovered tracers (mobile and immobile) or only with mobile tracers. High recovery rates ensure that the statistics from recovered tracers are representative of the whole tracer cloud, and we assume it is also representative of the true bedload dispersion of the investigated grain-sizes. When the proportion of lost tracers is high ($>20\%$), it is not possible to make sure that the true distribution of travel distances has been correctly approached by recovered tracers, unless an

independent observation of the tracer plume leading front is available, like, for example, a sediment wave reconstruction from topographic differencing (e.g., Arnaud et al., 2017; Brousse, Arnaud-Fassetta, et al., 2020). When low recovery rates are due to an important number of tracers being flushed downstream of the surveyed area, a truncation of the right-tail of the distance distribution occurs.

A compilation of recovery rates (including immobile tracers) from passive and active RFID studies shows a strong data scattering, from less than 10% to more than 90%, but most are above 60% (Figure 3a). Out of the four reported field experiments using the emerging technique of active UHF RFID, three were conducted in challenging large braided channels, with recovery rates systematically above 70% (Brousse, Arnaud-Fassetta, et al., 2020; Brousse, Liébault, et al., 2020; Misset et al., 2020). Active UHF RFID tags recently deployed in a meandering wide and deep aquatic channel showed contrasted results, with recovery rates ranging between 5 and 100%; low recovery rates have been interpreted as a consequence of large mining pits where many tracers may have been trapped and where surveys with RFID antenna were not possible (Boutault, 2020).

A rapid decline of passive RFID recovery rates for active channel width above 60 m is observed (Figure 3a). Values reported for large rivers are almost always below 45%, while those obtained for small streams commonly stand above 60%. However, tracer detection can be challenging even in small streams, notably in snowmelt or glacial-melt headwaters dominated by boulders and large woody debris, making survey difficult (e.g., Ivanov et al., 2020; Mao et al., 2020; Schneider et al., 2014). Another exception to the general trend is the tracing experiment of the wandering San Juan River in British Columbia, where the combination of portable antennas with different sizes allowed achieving recovery rates of PIT tags up to 75% in a 100-m wide active channel (McQueen et al., 2021).

FIGURE 3 Recovery rates (a) and number of recovered tracers (b) of passive and active RFID bedload surveys as a function of river channel width from data compilation of field studies (see Table S1). Vertical lines represent the range of reported values from multi-surveys at a given site; points represent values from single surveys at a given site.



The quality of a tracer dataset also depends on the absolute number of mobile recovered tracers. Although there is no rule of thumb for the sample size of tracer studies available in the literature, it clearly appears that low recovery rates obtained in large rivers have been compensated by the seeding of larger tracer populations, leading to equivalent mean sample sizes in small and large rivers (Figure 3b). Another recent strategy is based on a mixing of active and passive RFID to better capture frontrunners with active RFID (due to their generally high recovery rate) while maintaining a high number of recovered tracers with passive RFID (Boutault, 2020). A bootstrapping (with replacement) procedure has been proposed to estimate the geopositioning error of tracer cloud centroids as a function of the resampling rate of recovered tracers (Piégay et al., 2016). This approach can be useful for optimizing the sample size of tracer studies. The example of the large (100 m wide) Rhine River shows a geopositioning error of 10 m with a population of only 135 tracers at seeding time t_0 , when the tracer cloud is dispersed along a 600-m long channel reach (Figure 4; note that the y-axis is logarithmic). This error is however increasing through time (t_1 to t_4), showing that the required sample size for maintaining a geopositioning error of 10 m is increasing with tracer cloud diffusion.

Losses of tracers are of two types: (i) those inducing a definitive loss, like tracer breaking during transport or dispersion beyond the survey area, and (ii) those for which a re-appearance of tracers can be expected, like temporary storage in no-detection zones of the channel (deeply buried tracers or tracers located in inaccessible areas of the channel, like deep water zones or large accumulations of in-channel woods) or tracer clustering (signal collision effect for PIT tags). When multi-surveys are available, it becomes possible to determine the re-emergence rate of tracers, which has to be very low in case of definitive loss (Liébault et al., 2012; Schneider et al., 2014). A low re-emergence rate is generally a good indicator of tracers travelling beyond the study area, as confirmed by flume experiments showing that stones equipped with tags do not have a higher propensity to break during transport (Cassel, Piégay, et al., 2017). Comparative analysis of lost and recovered tracers with respect to grain-size or initial

position can also be helpful to evaluate the risk of missing frontrunners in the population of lost tracers (Chapuis et al., 2015; Liébault et al., 2012) and therefore to determine if field surveys should be extended downstream. Moreover, the re-emergence rate can also be an indicator of bedload transport conditions related with morphodynamics and flood sequencing (scour and fill processes). A toolbox was recently developed for maximizing information from a series of tracer surveys by better considering the effect of missing tracers on sediment displacement metrics (McVicar & Papangelakis, 2022).

3 | PHYSICAL PROCESSES OF BEDLOAD TRANSFER IN GRAVEL-BED RIVER CHANNELS

3.1 | Tracer transport distances and virtual velocity

3.1.1 | General observations on transport distances

The space–time domain of bedload tracing can be represented by a diagram of the maximum distance of transport (equivalent to the length-scale of bedload dispersion) versus the duration of the inter-survey period (period between two tracer surveys). This diagram (Figure 5a) clearly shows that the space–time domain of magnetic bedload tracing has been strongly stretched towards rapid bedload dispersion by RFID tracers. Although the longest monitoring period for magnets (17 years; Haschenburger, 2013) is still twice longer than for RFID (8 years; Bradley, 2017), the spatial scale of RFID experiments includes many tracer plumes with km-length scales, some of them having been obtained for very short inter-survey periods (e.g. Misset et al., 2020). Such extensive tracer plumes with magnets (maximum distance >1 km) are quite rare and correspond to long-term experiments (Ferguson et al., 2002; Haschenburger, 2013). To the best of our knowledge, the only reported cases of rapid bedload dispersion in the ‘before RFID’ tracing literature were obtained from

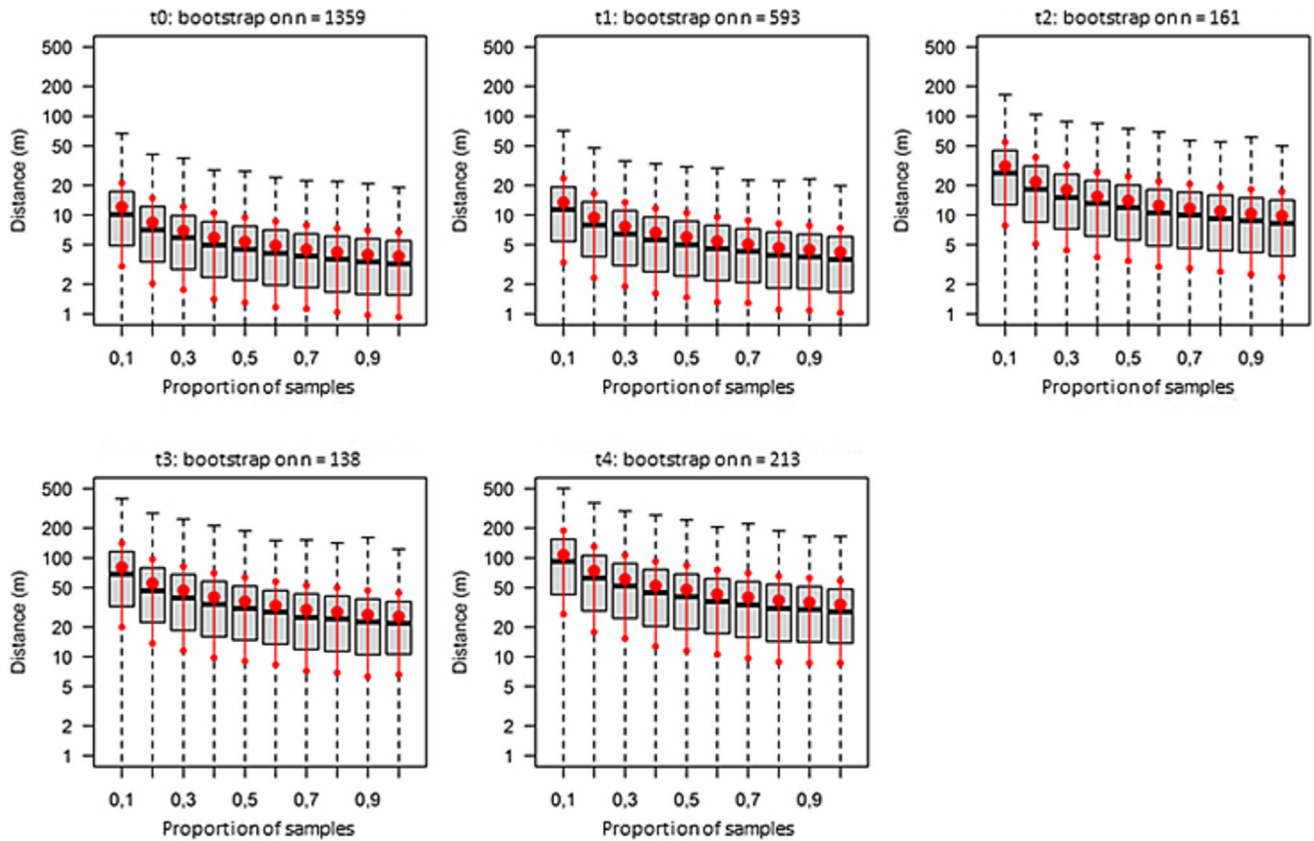


FIGURE 4 Geopositioning error of tracer cloud centroid (distance between estimated and real positions of the centroid, represented in y-axis) as a function of the number of resampled particles by a bootstrapping procedure with replacement. The five charts correspond to the tracer cloud at seeding time (t0) and after four successive surveys (t1 to t4) conducted on the Rhine River. The large red points correspond to the mean and the two small ones are the standard deviation (adapted from Piégay et al., 2016).

exotic tracers in a New Zealand braided stream (maximum transport distance of 1 km after a flow event of moderate intensity; Mosley, 1978) and in a small coastal gravel-bed river of California (maximum transport distance of 2.2 km after 3 years; Kondolf & Matthews, 1986).

Although the inter-survey period is arbitrary in that it depends on the timing of field surveys rather than accounting for hydrologic forcing that actually move grains, it provides a way to estimate the propagation rate of frontrunners (ratio between the maximum distance of transport and the inter-survey period, in m/year) and to look if a morphological pattern appears between fast- and slow-moving frontrunners. The gradient from supply- to transport-limited channel morphology proposed by Montgomery and Buffington (1997) was used to classify morphological types of compiled tracer surveys. This clearly shows that the proportion of transport-limited channel morphologies (riffle-pool single-thread and multi-thread) increases with the propagation rate of frontrunners (Figure 5b). It is interesting to note that braided channels (i.e., riffle-pool multi-thread) are systematically associated with very rapid frontrunners (>1 km/year). RFID tags, and particularly active UHF tags, have been very helpful for collecting data in such challenging fluvial environments (e.g., Brousse, Arnaud-Fassetta, et al., 2020; Brousse, Liébault, et al., 2020; Liébault et al., 2012; Misset et al., 2020), which were under-represented in the tracing literature based on painted or magnetic tracers. Other reported cases of rapid dispersion with RFID include a snowmelt stream with a plane-bed morphology (Olinde & Johnson, 2015) and a

by-passed channel of a large gravel-bed river (Arnaud et al., 2017; Chardon et al., 2021). These numerous examples clearly illustrate that RFID strongly improved the exploration of fluvial environments with rapid bedload dispersion.

Distributions of transport distances can be analysed through the relation between maximum and mean distances. A selection of all RFID and magnetic surveys with available information on recovery rates and number of recovered and mobile tracers was undertaken to look at this relation (Figure 6). The best fit was obtained with a power law having an exponent significantly <1 ($L_{\max} = 6.93 L^{0.85}$, with L_{\max} the maximum distance of transport, and L the mean distance of transport, $R^2 = 0.92$, 95% CI of exponent: 0.82–0.89, 95% CI of intercept: 6.07–7.91), meaning that the max/mean ratio is decreasing with the mean distance and therefore with flow intensity and/or duration of the tracer survey period. This also means that the central position of tracer plumes is moving faster over time than the position of tracer leading fronts. A possible explanation for this is that the burial depth of tracers increases with the distance of transport, but this needs to be confirmed by data. This is in agreement with several long-term observations of tracer dispersion (Bradley, 2017; Houbrechts et al., 2015) but not with some others showing a constant max/mean ratio through time (Haschenburger, 2013) or a leading front moving faster than the tracer plume centroid (Chardon et al., 2021). The former was explained by a size-selective effect, the front being composed of finer and more mobile tracers, while the latter was explained by a fragmentation of the tracer plume. Effects of recovery rate and

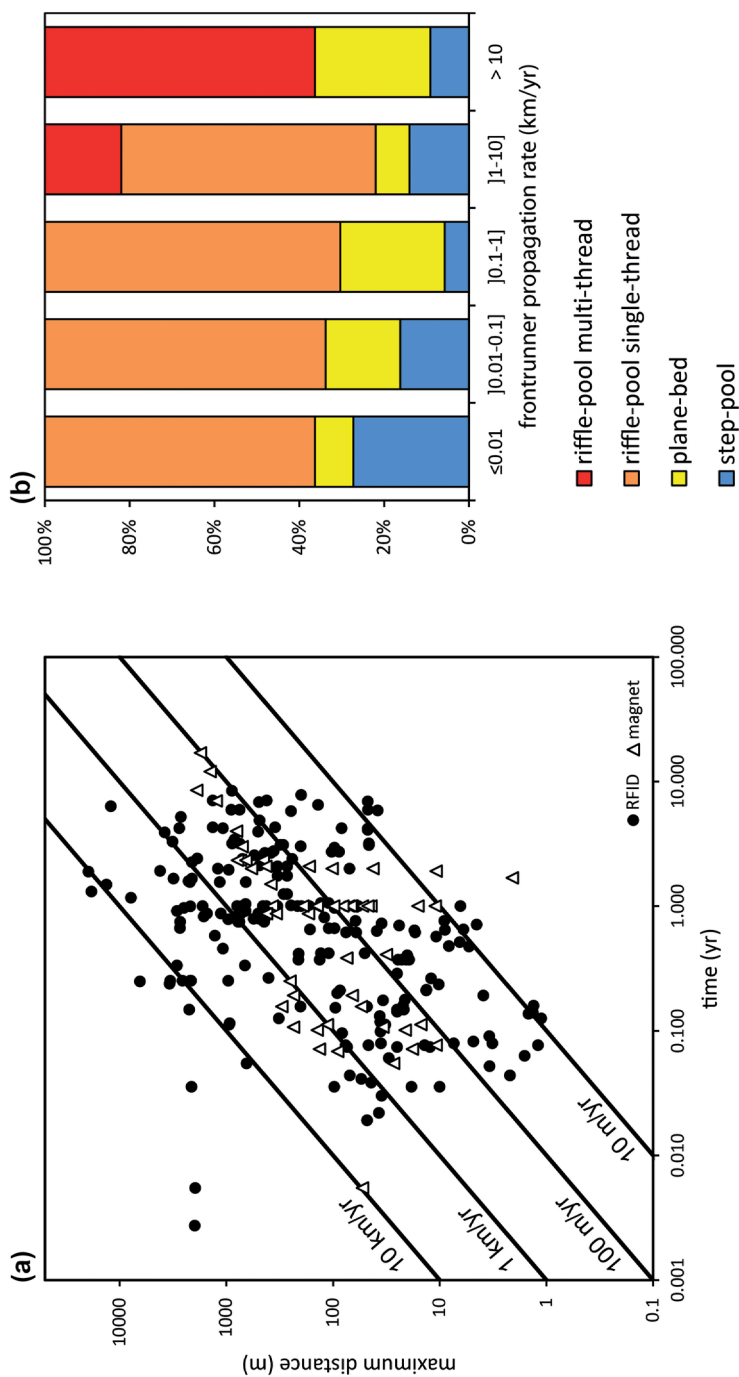


FIGURE 5 (a) Space-time domains of RFID and magnetic tracing experiments based on a meta-analysis of tracer surveys compiled from the literature (see Tables S1 and S2), including all inventories for which information on frontrunners (maximum distance) and survey periods (dates of tracer injections and surveys) are available ($n = 207$ for RFID and $n = 55$ for magnets); (b) distribution of morphological types as a function of frontrunner propagation rate derived from the maximum distance of transport over the inter-survey duration.

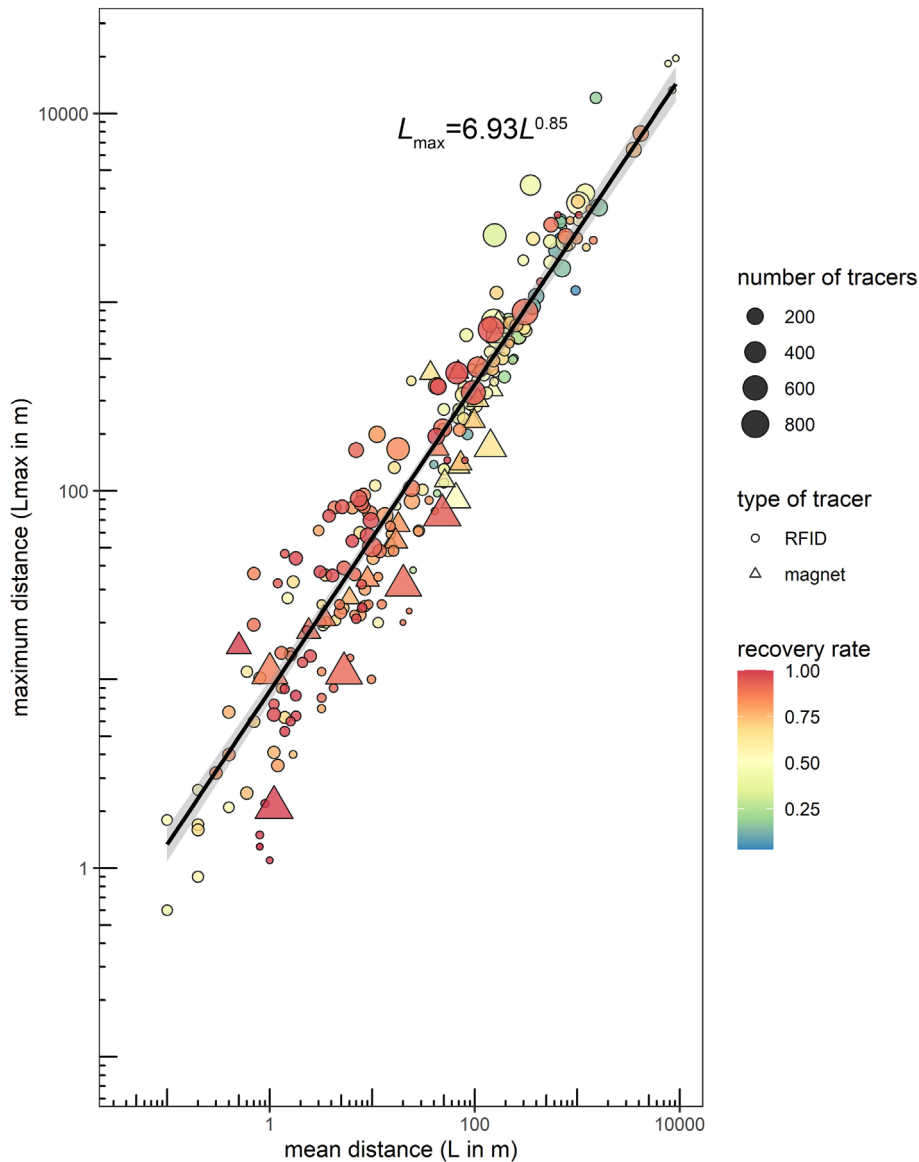


FIGURE 6 Scaling law between maximum and mean distances of transport of bedload tracing experiments based on a meta-analysis of tracer inventories from the literature (see Tables S1 and S2). The scatterplot includes all tracer surveys with available information on recovery rates and number of recovered and mobile tracers ($n = 214$ for RFID and $n = 29$ for magnets). The power law fit is based on the whole dataset ($n = 243$). The grey shading corresponds to the 95% confidence interval of the regression.

number of recovered tracers on the max/mean relation are low; these two quality factors do not show any clear positive or negative residual patterns with respect to the best fit. This means that the tracer leading front can be well detected with low recovery rates and/or small populations of recovered tracers.

3.1.2 | Effects of flow conditions on transport distances

One of the primary controls of bedload dispersion is hydraulic forcing. Excess specific stream power was early used in meta-analysis of tracer datasets for scaling the mean distance of transport with flow conditions (Hassan et al., 1992; Sear, 1996). This was done by considering the peak discharge between two tracer surveys relatively close in time. Many scaling laws of that type have been reported from event-based RFID tracing studies in different fluvial environments (Arnaud et al., 2017; Gilet et al., 2020; Houbrechts et al., 2015; Lamarre, Roy, 2008b; Papangelakis, McVicar, et al., 2019; Peeters et al., 2021; Rainato et al., 2020; Schneider et al., 2014). The excess stream power diagram from the meta-analysis of Hassan & Bradley (2017) was

updated with additional event-based surveys from our data compilation (Figure 7a). The morphological gradient appearing in fig. 6.1 of Hassan and Bradley (2017) is confirmed, with higher transport distances for transport-limited conditions (riffle-pool > plane-bed > step-pool). Significant statistical relationships have been obtained for each morphological group (Table 2), but with a very high intra-group scatter, typical of the variability of bedload responses to flow conditions. Additional factors of variability are related to morphological effects on bedload dispersion (see Section 3.1.4). It is interesting to see that many RFID datasets in riffle-pool channels plot within the gravel-over-sand group from magnets, which draws an upper envelope of bedload dispersion. This is another example showing the interest of RFID for documenting rapid bedload dispersion in gravel-bed rivers.

Normalization of transport distance can be valuable not only for comparing bedload dispersion of different morphological types but also for collapsing data along a single functional relation. By considering the mean step or riffle spacing as the normalization factor of the mean transport distance, a meta-analysis from Vázquez-Tarrio et al. (2019) showed a higher relative bedload mobility for step pools, as compared to riffle pools. Empirical relations obtained with dimensionless stream power were also improved with normalized data. Our data

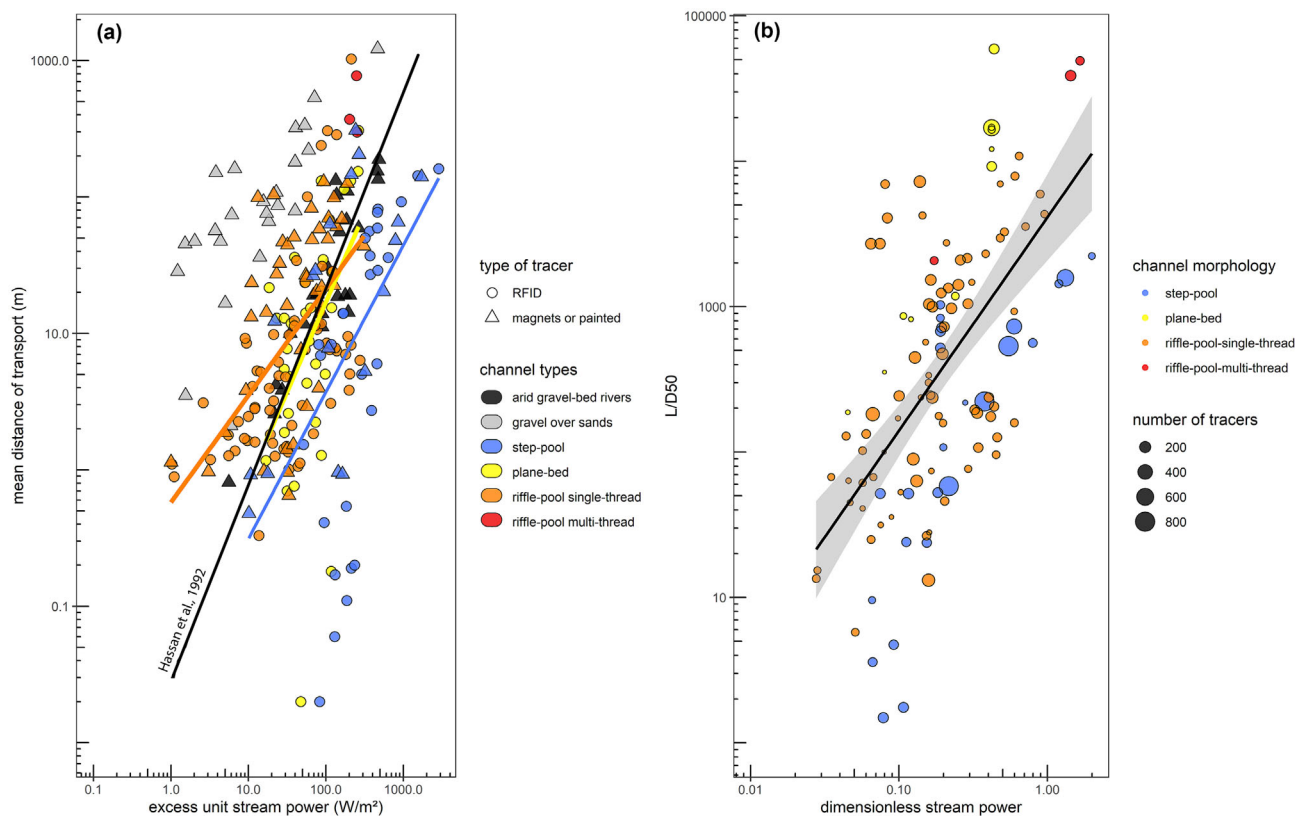


FIGURE 7 Stream power scaling laws from data compilation of bedload tracing surveys: (a) updating of the scatterplot from Hassan and Bradley (2017) between the mean distance of transport and the excess unit stream power, including tracing datasets collected in step-pool (Gintz et al., 1996; Lamarre & Roy, 2008b; Lenzi, 2004; Rainato et al., 2020; Schneider et al., 2014), plane-bed (Gilet et al., 2020; Houbrechts et al., 2015) and riffle pool channels (Arnaud et al., 2017; Haschenburger & Church, 1998; Houbrechts et al., 2015; Liébault et al., 2012; Papangelakis, McVicar, et al., 2019; Peeters et al., 2021; Plumb et al., 2017; Sear, 1996). Arid gravel-bed rivers and gravel-over sands correspond to data reported in Hassan et al. (1992). The black line represents the power law scaling of Hassan et al. (1992). Power law scaling obtained for step-pools, plane-beds and riffle-pools are represented in blue, yellow and orange, respectively. (b) Normalized mean distance of transport (L/D_{50} , with L the mean distance of transport, and D_{50} , the median grain-size of the channel surface) as a function of the dimensionless stream power computed for the D_{50} (Eaton & Church, 2011). This scatterplot includes compiled RFID and magnetic tracer surveys with available information on the number of mobile and recovered tracers, for which it has been possible to calculate the dimensionless stream power (see Tables S1 and S2). Datasets with inter-survey duration >1 year or with number of recovered and mobile tracers <30 were excluded. The black line represents the best fit, with 95% confidence interval of the regression in grey.

TABLE 2 Summary statistics of linear regressions on log-transformed values of mean distance of transport versus excess unit stream power using data presented in Figure 7a.

	Step pools	Plane beds	Riffle pools
Best fits	$L = 0.026 (\omega - \omega_0)^{1.076}$	$L = 0.039 (\omega - \omega_0)^{1.315}$	$L = 0.578 (\omega - \omega_0)^{0.784}$
95% confidence interval of intercepts	0.001–0.440	0.001–1.462	0.179–1.869
95% confidence interval of exponents	0.559–1.594	0.455–2.175	0.478–1.089
R^2	0.28	0.28	0.34
p value	<0.001	0.0038	<0.001
N	47	35	54

Note: L : mean distance of transport (m); $\omega - \omega_0$: excess unit stream power (W m^{-2}).

compilation allows investigating two normalization factors of bedload dispersion: channel width and median grain-size of the channel surface. Both allow a normalization by channel size, with an increase of channel width and a decrease of grain-size with drainage area. The dimensionless stream power of Eaton and Church (2011) was used as the flow predictor of the normalized distance of transport. This was computed as

$$\omega^* = \omega / \rho (gRD_{50})^{3/2}, \quad (1)$$

with ω the unit stream power, g the acceleration of gravity, ρ the water density, R the submerged specific gravity of sediment and D_{50} the median surface grain-size of the channel.

The best empirical relation was obtained with the transport distance normalized by the median channel grain-size ($L/D_{50} = 4954$

$\omega^{*1.66}$, $R^2 = 0.38$, p value < 0.001 , 95% CI of exponent: 1.27–2.05, 95% CI of intercept: 2355–10 415 (Figure 7b). This relation is based on a subset of surveys with populations of mobile and recovered tracers >30 . Tracer surveys associated with long time periods (inter-survey duration > 1 year) were also excluded in order to consider only surveys for which tracer mobility can be reasonably associated with one peak discharge. This analysis reveals contrasted patterns of bedload dispersion between morphological groups, with a lower relative bedload mobility in step pools, contrary to what has been obtained by Vázquez-Tarrío et al. (2019). Braided and plane-bed channels show the highest normalized bedload mobility. Plane-bed datasets with very high mobility correspond to a coarse mountain stream of Idaho (Olinde & Johnson, 2015), where a plausible explanation of extreme travel distances is the low vertical mixing of tracers during the survey period. Although most of riffle-pool single-thread channels show a high relative bedload mobility, many of them are characterized by a low bedload dispersion, comparable to step pools. A possible explanation for this variability is a strong heterogeneity of sediment supply conditions among this morphological group, which is composed of very different geomorphic settings, from strongly eroded upland catchments in alpine environments to lowland streams draining stable catchments. This also means that the classification of channel morphology used here as an indicator of sediment regime (supply vs transport-limited) is may be too rough to account for the gradient of sediment supply conditions of the compiled study sites. Of particular interest would be to test quantitative proxies of sediment supply based on the Shields number, as proposed by Church (2006), but this implies collecting more information about dominant flood discharges (bankfull discharges or 2-year flood discharges) of the study sites.

It remains quite uneasy to collapse the data along one single relation. A better collapsing should be possible by considering the full hydrological forcing during periods between tracer surveys, as proposed by Phillips et al. (2013), who introduced the concept of the dimensionless impulse for analysing tracer datasets. This approach was already successfully tested on several RFID tracer plumes (Arnaud et al., 2017; Chardon et al., 2021; Gilet et al., 2020; Imhoff & Wilcox, 2016; McQueen et al., 2021; Olinde & Johnson, 2015; Peeters et al., 2021; Plumb et al., 2017; Schneider et al., 2014), and a meta-analysis of those data would be certainly very instructive. Hydrological time series must be shared for making this possible, which is currently not the case for most of reported tracer surveys. Whatever the efforts that could be made for better characterizing hydrological and geomorphic predictors of transport distances, we should also be aware that data scatter is also related to many experimental factors related to the design of the tracing experiment in the field, highlighting the importance to provide a comprehensive methodological description in reported case studies.

3.1.3 | Grain-size and shape effects on bedload tracer mobility

Early bedload tracer studies have investigated the effects of particle size (Church & Hassan, 1992; Ferguson & Wathen, 1998) and shape (Schmidt & Ergenzinger, 1992; Schmidt & Gintz, 1995) on selective transport and sorting processes. Numerous RFID tracing experiments have pursued the exploration of size effects on transport distance

and/or virtual velocity (e.g., Dell'Agnese et al., 2015; Mao et al., 2020; McVicar & Roy, 2011; Rainato et al., 2018, 2020; Schneider et al., 2014). Those experiments provided field support to key theoretical findings relative to the physics of bedload transport, such as the equal-mobility concept (Parker et al., 1982) and partial and full mobility transport stages (Haschenburger & Wilcock, 2003; Wilcock & McArdell, 1993).

Investigations on partial and full mobility, focusing on entrainment or displacement phases, are based on two approaches, respectively: (i) the ratio of the number of mobile tracers to the number of recovered tracers (Casserly et al., 2020; McVicar & Roy, 2011; Papangelakis, McVicar, et al., 2019; Plumb et al., 2017) and (ii) the normalized relation of Church and Hassan (1992) between transport distance and particle size (referred as the CH92 relation) revisited by Vázquez-Tarrío et al. (2019). The mobility rate is computed for each grain-size class and compared between flood events of contrasted intensity. Repeated surveys allow fostering a range of discharges for the mobilization of the tracers and proposing probability curves of mobility depending on flow velocity for the investigated grain sizes (Chardon et al., 2021). The CH92 scaling procedure and their hybrid forms are based on a normalized transport distance (L_i/L_{D50} , with L_i the mean distance of the size group i , and L_{D50} the mean distance of the size group including the median surface grain-size of the bed material) and a normalized grain-size (D_i/D_{50} , with D_i the tracer grain-size, and D_{50} the median grain-size of the surface or subsurface bed material). The CH92 scaling law exhibits an exponential decreasing form. Most of the RFID tracing datasets showed good agreement with the CH92 relation, with full mobility (i.e., the transport distance is independent of grain size) for grain sizes up to two to four times the D_{50} (Casserly et al., 2020; Chardon et al., 2021; Mao et al., 2020; McVicar & Roy, 2011; Papangelakis, McVicar, et al., 2019; Plumb et al., 2017; Rainato et al., 2020; Schneider et al., 2014). Some field experiments also revealed that the size effect on tracer mobility can increase through time, due to possible changing channel conditions promoting partial mobility regime, notably in the specific case of gravel augmentation where starvation conditions rapidly prevail (Chardon et al., 2021).

Investigations on shape-selective transport using RFID tracers are rare and restricted to flume experiments (Cassel, Lavé, et al., 2021; Cassel, Piégay, et al., 2017). These authors demonstrated that the effect of particle shape was larger than the effect of particle density. A quantification of the shape-selective entrainment and transport was proposed, with recommendations for inclusion in bedload transport models. Field validations are needed to empirically address the complex dependency of the selective transport on bed-particle shape (Komar & Li, 1986), angularity (Li & Komar, 1986) and size (i.e., bed roughness) (Carling et al., 1992).

The size- and shape-selective transport along with abrasion process both contribute to the downstream fining trend formulated by Sternberg (1875), but their respective contributions have been long debated (Paola et al., 1992; Parker, 1991a, 1991b). The field application of a self-similar sorting profile concept (Paola & Seal, 1995) using a large population of RFID tracers in a tropical plane-bed river showed how a downstream fining can emerge after a short series of floods with slight size-dependent effects on sediment entrainment (Phillips & Jerolmack, 2014). Recent studies combining RFID monitoring and particle roundness measurement toolbox (Cassel et al., 2018; Cassel,

Piégay, et al., 2017) compared through a space-for-time substitution approach the abrasion and roundness trends obtained during lab experiments and a field survey in a volcanic gravel-bed river. Both field and flume tracer data support strong abrasion effects during the first kilometres of travel.

3.1.4 | Morphological controls on tracer dispersion

Travel distances of bedload particles during floods are not only controlled by flow conditions and grain size but also by channel morphology. Field evidences of morphological length scale effects on travel distances were obtained from RFID tracer plumes in step-pool streams (Lamarre, Roy, 2008b; Mao et al., 2020) and a bar-dominated river channel (McQueen et al., 2021). The paper by McQueen et al. (2021) showed that annual displacements of tracers deployed in the large wandering San Juan River were restricted to less than one riffle-pool-bar unit. A much faster bedload dispersion was observed in a similar channel morphology, where the mean annual travel distance can represent up to five to seven times the mean length of riffle-pool-bar units (Liébault et al., 2012). This length can be considered as

proportional to the channel width (Keller & Melhorn, 1978), which can therefore be seen as a controlling factor of annual travel distances of tracers (Beechie, 2001). Our data compilation confirms a general relation between the mean annual travel distance and the channel width (Figure 8). The best fit was obtained with a power law ($T = 1.4 w^{1.16}$, $R^2 = 0.40$, p value < 0.0001, with T the mean annual travel distance in m/year, and w the channel width, 95% CI of exponent: 0.94–1.38, 95% CI of intercept: 0.72–2.70). This relation was obtained by considering medium to long-term tracer surveys (inter-survey duration >0.5 years) to exclude event-based surveys for which the extrapolation of travel distances to the annual scale may not be representative. It is interesting to see that annual travel distances of most of the riffle-pool datasets are effectively less or equal to the typical length of the riffle-pool-bar unit (considered here as equal to 5.9 the channel width, as proposed by Keller & Melhorn, 1978). However, several riffle-pool datasets show that the annual travel distance can strongly exceed this length scale, and this is especially the case of the multi-thread riffle-pool group. Morphological controls on bedload dispersion in riffle-pool channels are more or less efficient depending on other factors, the sediment supply being likely a key forcing to consider. As previously said, the integration of quantitative proxies of sediment

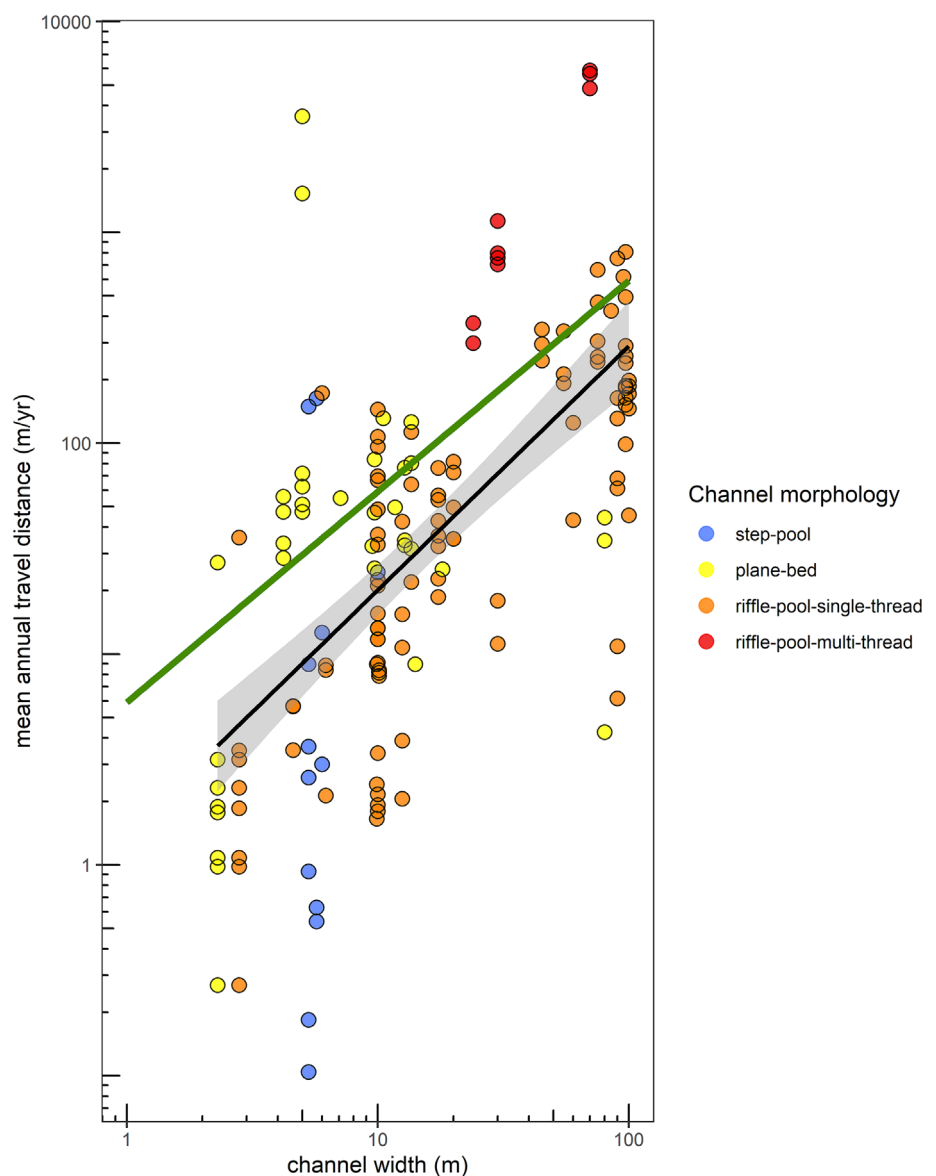


FIGURE 8 Mean annual travel distance as a function of the channel width. This scatterplot includes all compiled RFID and magnetic tracer surveys with available information on the duration of the inter-survey period and the mean travel distance (see Tables S1 and S2). Datasets with inter-survey duration <0.5 years were excluded. The black line corresponds to the best fit. The grey shading corresponds to the 95% confidence interval of the regression. The green line corresponds to the mean length of riffle-pool-bar units, considered as equal to 5.9 times the channel width (following Keller & Melhorn, 1978).

supply should potentially improve our understanding of the high variability of annual travel distances reported in tracer studies.

Morphological controls can also be considered by looking at the effect of initial conditions on tracer dispersion. Comparison of transport distances of tracers deployed in different morphological units generally shows a significant effect of initial conditions, with a stronger mobility of tracers deployed near or in low-flow channels, as compared to those deployed on gravel bars (Brenna et al., 2019; Chapuis et al., 2015; Liébault et al., 2012; McQueen et al., 2021). This has direct implications for spatial designs of tracer seeding, which can strongly influence statistics of displacement lengths. A recent work also showed how linear mixed modelling can be used for untangling controls on tracer mobility, such as the distance to the thalweg or to large woody debris (Clark et al., 2022). A reduction of the probability of entrainment as well as a reduced transport distance for tracers located close to large wood were demonstrated with this statistical modelling approach.

Several RFID experiments were also dedicated to interactions between bedload transfer and morphodynamics of riffle-pool-bar-units, generally by combining tracer data with 2D or 3D hydraulic modelling and/or with high-resolution topographic differencing data (Arnaud et al., 2017; Brousse, Arnaud-Fassetta, et al., 2020; Chapuis et al., 2015; McDowell et al., 2021; McQueen et al., 2021; Milan, 2013). Such intensive reach-scale monitoring has been very useful for interpreting morphological processes such as bar downstream migration or lateral accretion in terms of individual particle deposition and burial (McQueen et al., 2021). These morphological effects are known to produce multi-modal path length distributions that can be reproduced by Bayesian survival process models, as recently demonstrated with several RFID datasets (McDowell et al., 2021; McDowell & Hassan, 2020).

3.2 | Time-integrated mass fluxes and incipient motion

3.2.1 | Assessing bedload flux using the virtual velocity approach

A common strategy to assess bedload flux is to combine virtual velocity at the event time-scale with an active (scour-and-fill) sediment layer estimate, following the time-integrated bedload flux formula (Haschenburger & Church, 1998; Liébault & Laronne, 2008; Mao, Picco, et al., 2017):

$$G_b = v_b d_s w_s (1 - p) \rho_s, \quad (2)$$

where G_b is the bedload flux (kg s^{-1}), v_b is the mean virtual velocity of bed material (m s^{-1}), d_s the depth of the active layer (m), w_s the active width (m), p the porosity of bed material and ρ_s the sediment density (kg m^{-3}). The active width is defined as the bed portion over which bedload transport occurs. RFID tracers can be used to estimate both v_b and d_s .

In armoured-bed contexts, this approach can lead to notable underestimation of bedload transport, as the travel distance is estimated from the coarse particles in which RFID tags can be inserted, and it does not take into account finer elements such as the sandy

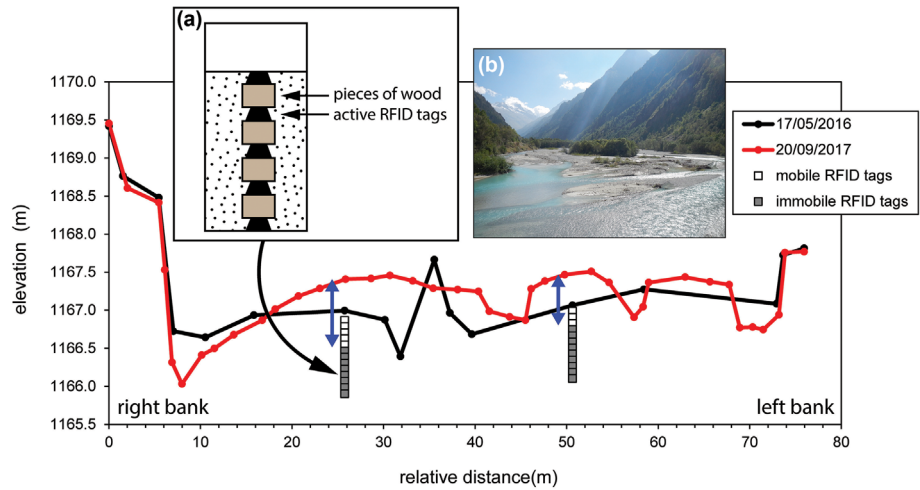
portion of the bedload or the small gravels, which are mobilized when the armour layer is broken-up (Houbrechts et al., 2012).

Virtual velocity is calculated from individual positions of tagged particles from two surveys done before and after the flow event, respectively. The tracers used to determine travel distances must be representative of the sediment transported within the active layer. The virtual velocity can also be estimated for the tracer cloud centroid when many PIT tags are injected (e.g., Chardon et al., 2021). The time period during which particles are virtually in motion has to be determined. Near-critical events during which only very few RFID tracers move over very short distances can be used to determine the critical discharge (e.g., Phillips & Jerolmack, 2014; Pangelakis, McVicar, & Ashmore, 2019). More commonly, authors perform hydraulic calculation of incipient motion based on the Shields formula. Daily surveys of passive RFID tags (Mao et al., 2020) and active UHF RFID stationary antenna (Cassel et al., 2023; Cassel, Navratil, et al., 2021) are alternative solutions for direct measurements of the virtual velocity.

Once the virtual velocity is calculated, the next step is to determine the active layer thickness. Different approaches have been proposed. Some only consider scour depth (e.g., Boutault, 2020), whereas others average the scour and fill depths (e.g., Brousse, Liébault, et al., 2020; Haschenburger & Church, 1998; Liébault & Laronne, 2008) or look at net elevation changes based on two successive topographic surveys (repetitive cross-sections or topographic differencing using Digital elevation models Of Difference, DoDs), providing a minimum estimate (e.g., Oss Cazzador et al., 2021). Scour and fill depths can be assessed by empirical predictions based on flow conditions (Brenna et al., 2019; Casserly et al., 2020; Haschenburger, 1999; Houbrechts et al., 2012; Mao, Picco, et al., 2017; Vázquez-Tarrío, Piqué, et al., 2021) or by simply considering the active layer thickness as equivalent to the maximum diameter (b -axis) of the locally displaced particles (Dell'Agnese et al., 2015) or equivalent to the channel median grain-size (Mao et al., 2020). They can also be directly measured in the field with traditional scour chains (e.g., Brenna et al., 2019; Haschenburger & Church, 1998; Liébault & Laronne, 2008), but these devices imply considerable field efforts for excavation after flow events, and many scour chains can be lost in large rivers with thick active layer. An interesting alternative to scour chains was provided by active RFID columns (or RFID scour chains), which are composed of columns of active UHF RFID tags inserted vertically in the channel (Figure 9). The anti-collision protocol of active UHF tags makes possible the simultaneous detection of many tags located close to each other. It is therefore possible to use an antenna for the remote detection of all the tags that are still present in RFID scour chains after a flow, without the need to excavate the bed. They were first tested in a wide braided reach of the French Alps (Brousse et al., 2018) where they permitted detection of a 1-m thick active layer. They have been also successfully used in a large braided river (Brousse, Liébault, et al., 2020) and in a large meandering river (Boutault, 2020) for capturing active layer thickness and estimating time-integrated bedload yields. Another alternative strategy to scour chains is tracers including a non-intrusive measurement of burial depth. A first prototype has been recently developed based on RFID tags and a rotating inner mechanism, showing promising results for burial depths not exceeding 15 cm (Cain & McVicar, 2020).

The active width is also a critical variable with a range of survey techniques. It can be obtained from the combination of topographic

FIGURE 9 Example of using active UHF RFID tags to survey the active layer thickness (blue arrows) by inserting columns of active UHF RFID tags in the alluvial bed. RFID columns are used to detect the maximum bed scouring level, and cross-section topographic resurvey is used to measure sediment deposition. RFID columns have been made by stacking RFID tags and pieces of wood visible at Inset (a). Data have been obtained in a braided river channel (Vénéon River, Inset b) (adapted from Brousse et al., 2018).



differencing and tracer entrainment along cross-sections (e.g., Liébault & Laronne, 2008) or from the mapping of mobile tracer positions in the active channel after a flow event (e.g., Haschenburger & Church, 1998). An estimate of the portion of the bed surface that has been entrained during the period is another solution. This can be captured with painted plots, empirically calibrated with the dimensionless critical shear stress (Mao, Picco, et al., 2017) or considered equal to the mobility rate of RFID tracers (Casserly et al., 2020).

3.2.2 | Incipient motion studies

RFID tracers have been used for characterizing incipient motion conditions of bedload transport in the field (Petit et al., 2015). This can be achieved by considering the relation between the frequency of mobile tracers and hydraulic forcings for a series of tracer surveys. It was shown that this frequency scales linearly with the peak Shields stress computed for the D_{50} of the tracer population, providing a mean to determine the critical Shields number (Phillips & Jerolmack, 2014). A similar approach was used to evaluate the impact of urbanization on bedload mobility, showing no effect on critical shear stress (Papangelakis, McVicar, et al., 2019). Another approach is to look at the relation between grain size of mobile tracers and flow parameters for inferring size-specific entrainment thresholds. A power law between the mean b -axis of the 10 largest transported tracers and the maximum specific stream power was obtained from the application of this flow competence approach (Houbrechts et al., 2015). This was also tested in the Rio Cordon step-pool stream by considering the minimum discharge at which a given tracer size fraction was entrained, providing a power law very similar to the one obtained with the maximum size fraction of bedload transport for a series of flow events recorded by a bedload monitoring station (Rainato et al., 2020).

The question of incipient motion conditions can also be addressed at the scale of individual tracers, by comparing shear stress conditions experienced by mobile and immobile tracers. By computing the shear stress at initial tracer positions at the time of the peak discharge during a period between two tracer surveys and by considering two populations of tracers (mobile vs immobile), one can calculate the probability of grain entrainment as a function of shear stress. This was successfully done using 2D hydraulic modelling of a flow event

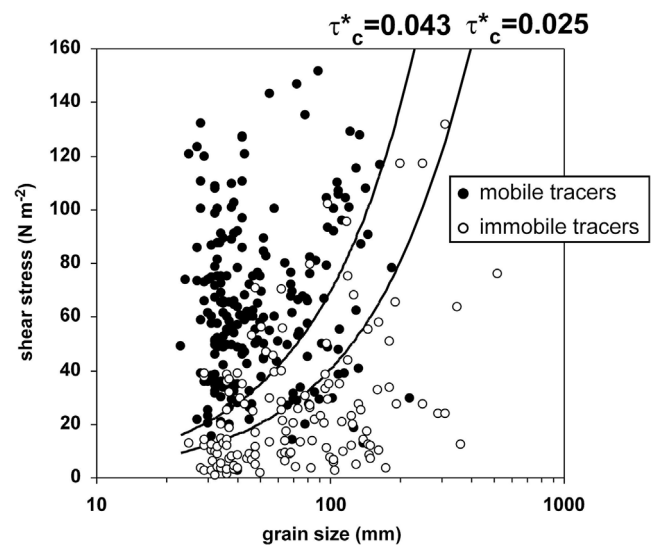


FIGURE 10 Peak shear stress experienced by mobile and immobile RFID tracers of the Bouinenc during the 2008 survey period (see Liébault et al., 2012, for details on the tracing experiment) as a function of grain-size; the two curves correspond to Shields numbers offering the best separation domain between mobile and immobile tracers.

mobilizing a large population of RFID tracers (Roberts et al., 2020). A simplified approach was used in the wandering Bouinenc gravel-bed river (RFID dataset presented in Liébault et al., 2012) by considering 1D shear stress computed from high-water marks along cross-sections of tracer seeding. The comparison of shear stress experienced by mobile and immobile tracers at the time of the peak discharge allows to propose a range of critical Shield numbers offering the best discriminant domain between the two groups (Figure 10).

4 | EVALUATING HUMAN EFFECTS ON BEDLOAD TRANSPORT USING RFID TAGS

Although RFID tracers have been early used to evaluate the physical effects of stream restoration (Biron et al., 2012; Carré et al., 2007), it is only from 2020 that applied studies took a prominent place (see Figure 1), with many case studies dealing with artificial gravel

augmentations or sediment continuity. Main findings from these two specific topics are summarized below, but other topics have been recently covered with RFID tracers, such as the impact of urbanization on bedload transport (Papangelakis, McVicar, et al., 2019; Plumb et al., 2017), riffle-pool restoration projects (Papangelakis & MacVicar, 2020) or side-channel restoration (Eschbach et al., 2021).

4.1 | Monitoring and predicting gravel augmentation effects

Sediment replenishment is becoming a common strategy for restoring incised river channels, and RFID tracers proved to be very useful for assessing the time needed for replenished sediment to exit the restored reach or for assessing volume and frequency of artificial sediment inputs. The first RFID application for monitoring gravel augmentation was undertaken in the lower Ain River downstream of the Allement dam, Eastern France (Piégay et al., 2016; Rollet et al., 2008). RFID tracking was used to survey transport distances of reintroduced gravels during 4 years, showing mean annual displacements ranging from 210 to 600 m, with frontrunners found 3770 m downstream of the seeding site. Similar field experiments were undertaken to monitor gravel augmentation in the Upper Rhine downstream of the Kembs dam (Arnaud et al., 2017; Chardon et al., 2021) and in by-passed reaches of the Rhône River (Vázquez-Tarrió, Arnaud, et al., 2021). On these two regulated gravel-bed rivers, very large populations of PIT tags ($n = 1000$ to 1500) were introduced in the replenished sediments with recovery rates of 11–43% for the Rhine and 7–67% for the Rhône. A replenished site of the Rhine has been surveyed seven times between 2009 and 2017, including a 15-year flood. Translation of the sediment pulse and then dispersion and fragmentation were observed through time, with preferential deposition on riffles (Figure 11; Chardon et al., 2021). A multiple regression model was applied to the Rhône dataset including 35 RFID surveys (Vázquez-Tarrió, Arnaud,

et al., 2021). It showed promising results to estimate mean transport distances, making it therefore possible to estimate the time needed to export a given volume of sediments from a restored river reach, as well as the volume potentially trapped in the reach. These results are essential to go further into optimal location, volume, geometry and sustainability of gravel augmentation operations related to local hydraulic conditions.

Stähly et al. (2020) reported another case study on the Sarine River in Switzerland. Four artificial deposits allocated as alternate bars were previously tested in a flume and then implemented in the field to evaluate the effects of a dam flood release. The experiment was useful to improve the design of flow hydrographs and of the deposits. It also showed that passive RFID-tagged particles were recovered in a repetitive pattern of clusters, leading to an increase in hydraulic habitat diversity, as expected from previous laboratory observations.

4.2 | Monitoring human effects on sediment continuity

The employment of RFID tracers for evaluating the effect of hydraulic structures (dams, weirs and check-dams) on the longitudinal sediment continuity is an emerging topic of the last 3 years, with several dedicated field experiments in gravel-bed rivers of Europe (Brenna et al., 2020; Brousse, Arnaud-Fassetta, et al., 2020; Casserly et al., 2020, 2021; Galia et al., 2021; Gilet et al., 2021; Peeters et al., 2020) and North America (Fields et al., 2021; Magilligan et al., 2021). This reflects the growing concern of water management policies (e.g., EU Water Framework Directive) in restoring the connectivity of fragmented fluvial reaches, which are now common with the multiplication of in-channel barriers (Belletti et al., 2020). Bedload transport studies are more and more engaged in applied research on grade-controlled river channels, with RFID solutions often included in the monitoring design. These studies provide not only field evidences

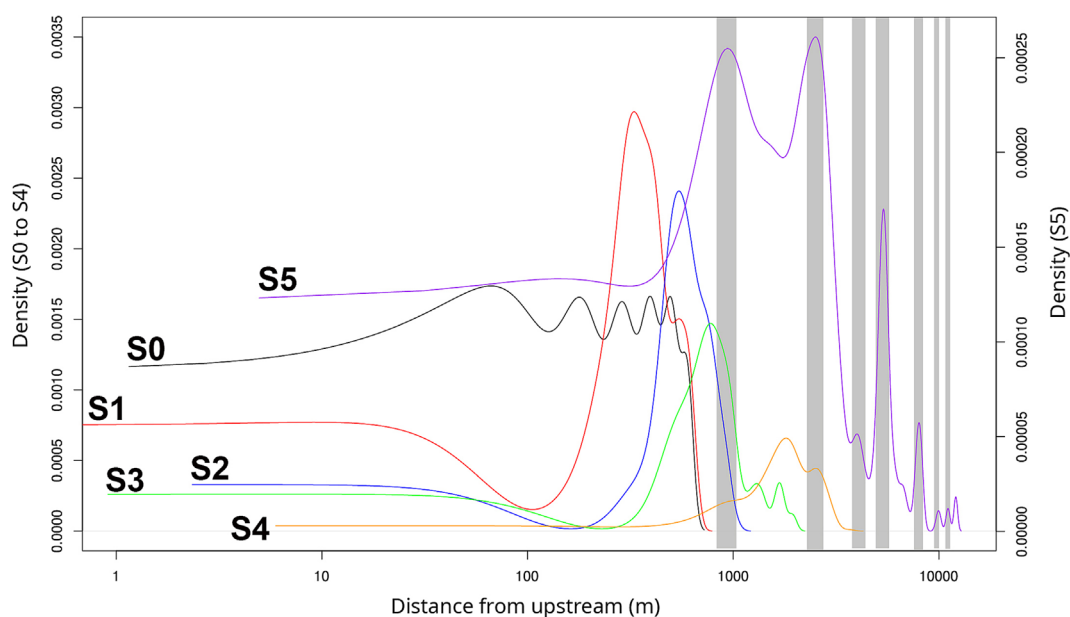


FIGURE 11 Probability density functions of the longitudinal position of RFID tracers recovered after five surveys in the Rhine River (S1 to S5; S0 corresponds to tracer seeding); grey columns correspond to riffles; note that the y-scale for S5 was adjusted for better visibility of the sediment wave fragmentation (from Chardon et al., 2021, modified by Chardon and Schmitt).

on the sedimentary effect of hydraulic structures but also interesting observations about what happens after their removal. Many being old and abandoned, their removal is often considered in river restoration projects. Such restoration works require strong scientific evidences of their potential benefits in terms of sediment continuity, since other socio-environmental issues may advocate for the conservation of abandoned structures, that is, the sequestration of contaminated sediments or the preservation of historical heritage (Peeters et al., 2020).

The trapping effect of dams on bedload transport may lead to dramatic alterations of the downstream channel morphology and associated freshwater habitats. This has been observed in a large gravel-bed river of the Northern Apennines, where a tracing experiment was undertaken to evaluate sediment starvation effects below a dam. PIT tags were used in combination with painted tracers to quantify the time-integrated bedload transport rate using the virtual velocity approach (Brenna et al., 2020). This study revealed a strong alteration of sediment mobility, with a longitudinal gradient of the dam effect, the most impacted reaches being those located closer to

the dam. One way to improve the passing of coarse sediments is to open hydraulic gates during floods (sluicing operation). Active RFID tracers deployed in a braided river of the Southern French Alps showed that around 20% of the injected tracers crossed the dam gates during a 5-year flood for which a full sluicing was operating (Brousse, Arnaud-Fassetta, et al., 2020) (Figure 12). PIT tags were also recently used to document the effect of dam removal in a gravel-bed river of NE France (Gilet et al., 2021) and showed that the bedload continuity has been efficiently restored, but the downstream channel morphology remained unchanged. Critical shear stress over the course of channel recovery following dam removal has been constrained with smart rocks equipped with PIT tags and accelerometers, providing evidences of the rapid post-removal formation of a threshold channel (Fields et al., 2021).

Although sediment starvation below dams can be seen as an obvious alteration of sediment continuity, this is much less clear for smaller grade-control hydraulic structures such as weirs (also referred as low-head dams or run-of-river dams) or check dams. The

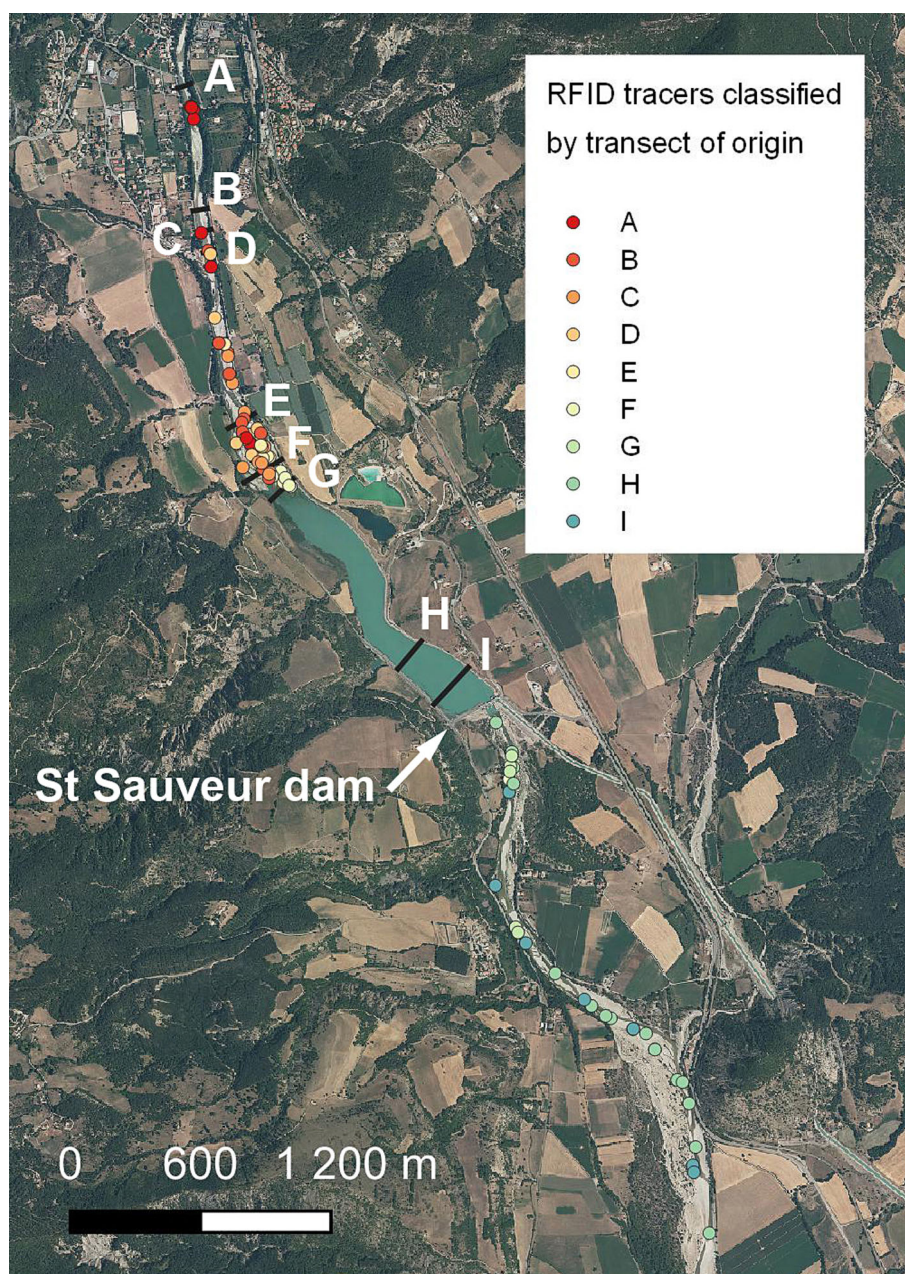


FIGURE 12 An example of active UHF RFID tracer dispersion after a 5-year flood in the Buëch River, SE France, attesting an efficient bedload transfer through the St Sauveur dam related to a sluicing operation; letters correspond to tracer seeding cross-sections; more information on this tracing experiment can be found in Brousse, Arnaud-Fassetta, et al. (2020).

sedimentary effect of weirs was investigated by seeding RFID tracers in two gravel-bed rivers of SE Ireland, revealing a state of transient storage with coarse particles ($>D_{90}$ of the riverbed) passing through weirs (Casserly et al., 2020). Tracer-derived fractional transport stages however suggest persistence of supply-limited conditions downstream from the structures. Similar conclusions were reported in a gravel-bed river of Belgium, strongly controlled by old abandoned weirs. Results showed that RFID tracers in the range of the channel D_{50} can pass the weir, suggesting that these structures can be considered as leaky barriers for sediment continuity (Peeters et al., 2020). RFID tracers deployed upstream and inside reservoirs controlled by weirs in several gravel-bed rivers of New England also revealed a high degree of sediment connectivity in grade-controlled reaches (Magilligan et al., 2021). More surprisingly, RFID tracers deployed in two mountain streams of Western Carpathians, one strongly controlled by check-dams, and one with a free riffle-pool-bar morphology, revealed that check dams act as boosters of longitudinal sediment connectivity, due to the strong bed armoring and the subsequent low vertical mixing of bedload tracers (Galia et al., 2021).

5 | KEY CHALLENGES OF RFID BEDLOAD TRACING

The various ways fluvial geomorphologists initially developed RFID tracking techniques to provide new knowledge, predict transport distances and diagnose river behaviour and responsiveness are inspiring in terms of collective intelligence because successive publications are steps to improve initial findings. A lot of progress has already been done; however, there are still rooms to improve the use of the techniques. Four key challenging issues can be stated.

1. Optimizing field and statistical protocols for RFID bedload tracing datasets

This includes methodological analysis of sample sizes required for different objectives, that is, assessing if n RFID tracers recovered are enough or not to achieve a robust reconstruction of transport distance distributions for different types of fluvial environments. Bootstrapping procedures on large populations of recovered tracers must be run in this way to better understand sample size effect on geopositioning errors. Tracer cloud geometry must also be evaluated to provide stronger indices of bedload transport representativity. Procedures to verify that frontrunners are well detected must be developed based on probabilistic functions. Strategies to include information from missing tracers should also be more systematically undertaken to increase the proportion of tracers used to calculate displacements metrics (McVicar & Papangelakis, 2022). The optimization of field protocols requires technological improvements to gain in RFID tracking efficiency (reduction of the survey time and increase of the recovery rate by improving both the performance of the tags and the survey strategies) and in representativeness of the tracers (reduce the size and the cost of the active tags to increase the grain size range and the sample sizes). Specifically, fluvial geomorphologists should share their procedures to avoid collision effects with passive RFID, increase detection ranges and recovery rates and reduce time in the field to reiterate surveys (with UAVs, active UHF tags notably).

2. Fostering the use of RFID tracers as a surrogate tool for bedload transport monitoring in the field

Methodological research towards the development of 'smart' RFID tracers is strategic for pushing forward tracer-based bedload monitoring solutions. This is particularly crucial for fluvial environments where direct bedload sampling techniques are difficult to use (e.g., large rivers and braided channels). A 'smart' RFID tracer that informs not only about distance of transport but also burial depth, resting time and step length would offer all the required information for quantifying bedload flux with the virtual velocity approach. A potential way to constrain RFID burial depth is to couple detection antennas for 3D geopositioning of tracers. This is now possible because we better understand the RFID emission cone and we can fix the PIT tag orientation within artificial particles (the Wobblestone tracer from Cain & McVicar, 2020). Real-time monitoring of virtual velocity is another promising way thanks to the use of permanent UHF antennas (Cassel, Navratil, et al., 2021). In glacial-melt or snowmelt flow regimes, daily tracer surveys with a mobile antenna allow approaching resting times and step lengths (Mao et al., 2020). Such field experiments based on high-frequency surveys or continuous monitoring of virtual velocity are still quite uncommon and should be replicated in the near future to confirm their interest for indirect bedload transport monitoring. Active UHF RFID tracers offer an efficient solution for bedload tracing and active layer measurement of large gravel-bed rivers, but more field experiments are needed for validating bedload flux estimates. There are also rooms to combine techniques such as active and passive RFID tracers to maximize the detection of frontrunners and tracer cloud centroids. The merging of RFID datasets with other sensors (e.g., seismic and acoustic sensors) offers a way to investigate moments and conditions of mobility at different spatio-temporal scales within the river reach (Misset et al., 2020). Smartrocks equipped with motion sensors (accelerometers) to infer the precise timing and duration of grain movements at high temporal resolution already exist (Gronz et al., 2016; Maniatis, 2021; Olinde & Johnson, 2015). Few field experiments have demonstrated their ability to capture thresholds of motion variability through time, as well as motion and rest durations (Pretzlav et al., 2020 and 2021). However, data from smartrocks could not be remotely collected in these studies, implying strong limitations in large or very active river channels, where both smartrock recovery and excavation can be quite challenging. Combining active UHF RFID with accelerometer into a smartrock is an attractive solution for this that still needs to be tested.

3. Using RFID tracers to investigate interactions between bedload transport and channel morphology

RFID tracers clearly have a role to play in reach-scale integrated approaches of gravel-bed river morphodynamics. The coupling of tracer dispersion with high-resolution topographic differencing data not only helps to understand basic process-form interactions of river channels (e.g., riffle-pool-bar maintenance as in Milan, 2013, or McQueen et al., 2021) but also contributes to exploration of the links between grain-scale mobility and macroform dynamics (e.g., bedload sheets and sediment waves, as in Arnaud et al., 2017, or Brousse, Arnaud-Fassetta, et al., 2020). Emerging stakes are also related to the modelling of tracer kinematics. The combination of numerical hydraulic modelling and RFID tracking is a promising solution for unifying

Eulerian and Lagrangian views of bedload transport. Although tracking is time-consuming in medium to large rivers so that the field effort is limited in space and time, it can provide a very valuable field validation framework for developing numerical simulations. Numerical modelling can inform on particle path characteristics with regards to morphology and flow hydraulics in the river reach (Biron et al., 2012; Chapuis et al., 2015; Milan, 2013; Roberts et al., 2020). Process-based laboratory experiments including RFID tracers have not been widely used so far and restricted to the study of abrasion rates (Cassel et al., 2018), particle shape-effect on mobility (Cassel, Lavé, et al., 2021) and process-form interactions (e.g. McDowell et al., 2021). Recent developments of a specifically designed flume for RFID tracking (Hufnagel & MacVicar, 2018) should foster laboratory experiments with RFID tracers.

4. Fostering future meta-analysis of RFID bedload tracing experiments

Meta-analyses are very valuable for predicting tracer transport distances and exploring the variability of bedload dispersion in heterogeneous fluvial environments. The compilation of RFID datasets delivered with this review paper allows us to share information of 459 tracer surveys for a total of 125 study sites encompassing a great variety of fluvial environments and flow regimes. To provide new results in this domain, there is clearly a collective organization to initiate in terms of standardization of data collection protocols and data sharing. Summary information is generally (but unfortunately, not systematically) provided by authors in primary research papers, for example, type of RFID tag, tracer particle GSD, seeding and survey dates, number of deployed tracers, recovery rates, mobility rates, mean and maximum travel distances, study site characteristics including bed slope, channel width and flood discharges (most of these terms are presented in our bedload tracing database; see the [supporting information](#)). Other data would be of great interest for future meta-analyses. For example, the systematic sharing of tracer coordinates and individual transport distances, as well as hydrological time series during tracing experiment, would open new perspectives and promote efforts on functional relationships for the prediction of bedload mobility going beyond site-specific scaling laws. In addition, information on the area of the surveyed surface, the way the survey was conducted through the GPS tracking lines, the antenna sizes, the time spent and the number of observers, would be of interest for assessing the sampling effort and quality. Fluvial geomorphologists have been very careful with the recovery rate in the emerging phase of RFID applications. We now need to combine the recovery rate with other quality criteria, such as the RFID survey density and the RFID recovery density to provide a spatial resolution of the survey and better identify the causes for tracer loss. The 'efficiency score' proposed by Cassel et al. (2020) is based on the surveying effort. It offers an interesting framework to discuss the overall cost of RFID tracing (including equipment and surveys) and therefore support users in the choice of an RFID technology and survey protocol adapted to their study site.

AUTHOR CONTRIBUTIONS

Conceptualization: Frédéric Liébault. **Investigation:** Frédéric Liébault, Hervé Piégay, Mathieu Cassel and Fanny Arnaud. **Resources:** Frédéric Liébault, Fanny Arnaud and Mathieu Cassel. **Supervision:** Frédéric Liébault. **Writing—initial draft:** Frédéric Liébault, Hervé Piégay,

Mathieu Cassel and Fanny Arnaud. **Writing—reviewing and editing:** Frédéric Liébault, Hervé Piégay, Mathieu Cassel and Fanny Arnaud.

ACKNOWLEDGEMENTS

Many RFID field experiments reported in this review paper have been undertaken in the framework of the LTER ZABR, CNRS-INSU-SNO Draix-Bléone, Rhône Sediment Observatory (OSR) programme, and EUR H2O'Lyon (ANR-17-EURE-0018) of Université de Lyon (UdL). The Draix-Bléone Observatory is funded by INRAE, CNRS-INSU and OSUG and is part of the French network of Critical Zone Observatories OZCAR, which is supported by the French Ministry of Research, French Research Institutions and Universities. David Milan, Louis Gilet and Fabien Boutault are acknowledged for personal communications about their RFID tracer datasets. Valentin Chardon and Laurent Schmitt are acknowledged for sharing Figure 11. We acknowledge the thorough reviews by Riccardo Rainato, Joel Johnson, Georgie Bennett, and two anonymous reviewers.

DATA AVAILABILITY STATEMENT

Data are available as [supporting information](#).

ORCID

Frédéric Liébault  <https://orcid.org/0000-0002-3155-6779>

Hervé Piégay  <https://orcid.org/0000-0002-3864-2119>

Mathieu Cassel  <https://orcid.org/0000-0001-6504-3990>

Fanny Arnaud  <https://orcid.org/0000-0002-8784-1384>

REFERENCES

- Arnaud, F., Piégay, H., Béal, D., Collery, P., Vaudor, L. & Rollet, A.J. (2017) Monitoring gravel augmentation in a large regulated river and implications for process-based restoration. *Earth Surface Processes and Landforms*, 42(13), 2147–2166. Available from: <https://doi.org/10.1002/esp.4161>
- Arnaud, F., Piégay, H., Vaudor, L., Bultingaire, L. & Fantino, G. (2015) Technical specifications of low-frequency radio identification bedload tracking from field experiments: differences in antennas, tags and operators. *Geomorphology*, 238, 37–46. Available from: <https://doi.org/10.1016/j.geomorph.2015.02.029>
- Beechie, T.J. (2001) Empirical predictors of annual bed load travel distance, and implications for salmonid habitat restoration and protection. *Earth Surface Processes and Landforms*, 26(9), 1025–1034. Available from: <https://doi.org/10.1002/esp.251>
- Belletti, B., Garcia de Leaniz, C., Jones, J., Bizzi, S., Börger, L., Segura, G., et al. (2020) More than one million barriers fragment Europe's rivers. *Nature*, 588(7838), 436–441. Available from: <https://doi.org/10.1038/s41586-020-3005-2>
- Biron, P.M., Carver, R.B. & Carré, D.M. (2012) Sediment transport and flow dynamics around a restored pool in a fish habitat rehabilitation project: field and 3D numerical modelling experiments. *River Research and Applications*, 28(7), 926–939. Available from: <https://doi.org/10.1002/rra.1488>
- Boutault, F. 2020. Etude de l'impact cumulé des facteurs d'anthropisation sur la Dordogne moyenne et préconisations en vue de la restauration écologique du cours d'eau. Unpublished PhD thesis, Université Jean Moulin Lyon 3, 215 pp.
- Bradley, D.N. (2017) Direct observation of heavy-tailed storage times of bed load tracer particles causing anomalous superdiffusion. *Geophysical Research Letters*, 44(24), 12227–12235. Available from: <https://doi.org/10.1002/2017GL075045>
- Bradley, N.D. & Tucker, G.E. (2012) Measuring gravel transport and dispersion in a mountain river using passive radio tracers. *Earth Surface Processes and Landforms*, 37(10), 1034–1045. Available from: <https://doi.org/10.1002/esp.3223>

- Brenna, A., Surian, N. & Mao, L. (2019) Virtual velocity approach for estimating bed material transport in gravel-bed rivers: key factors and significance. *Water Resources Research*, 55(2), 1651–1674. Available from: <https://doi.org/10.1029/2018WR023556>
- Brenna, A., Surian, N. & Mao, L. (2020) Response of a gravel-bed river to dam closure: insights from sediment transport processes and channel morphodynamics. *Earth Surface Processes and Landforms*, 45(3), 756–770. Available from: <https://doi.org/10.1002/esp.4750>
- Brousse, G., Arnaud-Fassetta, G., Liébault, F., Bertrand, M., Melun, G., Loire, R., et al. (2020) Channel response to sediment replenishment in a large gravel-bed river: the case of the Saint-Sauveur dam in the Buëch River (Southern Alps, France). *River Research and Applications*, 36(6), 880–893. Available from: <https://doi.org/10.1002/rra.3527>
- Brousse, G., Arnaud-Fassetta, G., Liébault, F. & Vázquez-Tarrió, D. (2018) Experimental bed active layer survey with active RFID scour chains: example of two braided rivers in the French Alps (the Drac and the Vénéon). In: *Proceedings of river flow 2018*. Lyon-Villeurbanne: WASER. <https://doi.org/10.1051/e3sconf/20184004016>
- Brousse, G., Liébault, F., Arnaud-Fassetta, G., Breilh, B. & Tacon, S. (2020) Gravel replenishment and active-channel widening for braided-river restoration: the case of the Upper Drac River (France). *Science of the Total Environment*, 766, 142517. Available from: <https://doi.org/10.1016/j.scitotenv.2020.142517>
- Cain, A. & McVicar, B. (2020) Field tests of an improved sediment tracer including non-intrusive measurement of burial depth. *Earth Surface Processes and Landforms*, 45(14), 3488–3495. Available from: <https://doi.org/10.1002/esp.4980>
- Carling, P.A., Kelsey, A. & Glaister, M.S. (1992) Effect of bed roughness, particle shape and orientation on initial motion criteria. In: Billi, P., Hey, C.R., Thorne, C.R. & Tacconi, P. (Eds.) *Dynamics of gravel-bed rivers*. Chichester: John Wiley and Sons, pp. 24–39.
- Carré, D.M., Biron, P.M. & Gaskin, S.J. (2007) Flow dynamics and bedload sediment transport around paired deflectors for fish habitat enhancement: a field study in the Nicolet River. *Canadian Journal of Civil Engineering*, 34(6), 761–769. Available from: <https://doi.org/10.1139/L06-083>
- Cassel, M., Dépret, T. & Piégay, H. (2017) Assessment of a new solution for tracking pebbles in rivers based on active RFID. *Earth Surface Processes and Landforms*, 42(13), 1938–1951. Available from: <https://doi.org/10.1002/esp.4152>
- Cassel, M., Lavé, J., Recking, A., Malavoi, J.R. & Piégay, H. (2021) Bedload transport in rivers, size matters but so does shape. *Scientific Reports*, 11(1), 508. Available from: <https://doi.org/10.1038/s41598-020-79930-7>
- Cassel, M., Navratil, O., Liébault, F., Recking, A., Vázquez-Tarrió, D., Bakker, M., et al. (2023) Assessment of pebble virtual velocities by combining active RFID fixed stations with geophones. *Earth Surface Processes and Landforms*, Available from: <https://doi.org/10.1002/esp.5646>
- Cassel, M., Navratil, O., Perret, F. & Piégay, H. (2021) The e-RFIDuino: an Arduino-based RFID environmental station to monitor mobile tags. *HardwareX*, 10, e00210. Available from: <https://doi.org/10.1016/j.ohx.2021.e00210>
- Cassel, M., Piégay, H., Fantino, G., Lejot, J., Bultingaire, L., Michel, K., et al. (2020) Comparison of ground-based and UAV a-UHF artificial tracer mobility monitoring methods on a braided river. *Earth Surface Processes and Landforms*, 45(5), 1123–1140. Available from: <https://doi.org/10.1002/esp.4777>
- Cassel, M., Piégay, H. & Lavé, J. (2017) Effects of transport and insertion of radio frequency identification (RFID) transponders on resistance and shape of natural and synthetic pebbles: applications for riverine and coastal bedload tracking. *Earth Surface Processes and Landforms*, 42(3), 399–413. Available from: <https://doi.org/10.1002/esp.3989>
- Cassel, M., Piégay, H., Lavé, J., Vaudor, L., Hadmoko Sri, D., Wibiwo Budi, S., et al. (2018) Evaluating a 2D image-based computerized approach for measuring riverine pebble roundness. *Geomorphology*, 311, 143–157. Available from: <https://doi.org/10.1016/j.geomorph.2018.03.020>
- Cassery, C.M., Turner, J.N., O'Sullivan, J.J., Bruen, M., Bullock, C., Atkinson, S., et al. (2020) Impact of low-head dams on bedload transport rates in coarse-bedded streams. *Science of the Total Environment*, 716, 136908. Available from: <https://doi.org/10.1016/j.scitotenv.2020.136908>
- Cassery, C.M., Turner, J.N., O'Sullivan, J.J., Bruen, M., Magee, D., O'Coiléir, S., et al. (2021) Coarse sediment dynamics and low-head dams: monitoring instantaneous bedload transport using a stationary RFID antenna. *Journal of Environmental Management*, 300, 113671. Available from: <https://doi.org/10.1016/j.jenvman.2021.113671>
- Chacho, E.F., Burrows, R.L. & Emmett, W.W. (1989) Detection of coarse sediment movement using radiotransmitters. In: *Proceedings XXIII congress on hydraulics and the environment*. Ottawa: International Association of Hydraulic Research, pp. 367–373.
- Chapuis, M., Bright, C.J., Hufnagel, J. & McVicar, B. (2014) Detection ranges and uncertainty of passive Radio Frequency Identification (RFID) transponders for sediment tracking in gravel rivers and coastal environments. *Earth Surface Processes and Landforms*, 39(15), 2109–2120. Available from: <https://doi.org/10.1002/esp.3620>
- Chapuis, M., Dufour, S., Provansal, M., Couvert, B. & de Linares, M. (2015) Coupling channel evolution monitoring and RFID tracking in a large, wandering, gravel-bed river: insights into sediment routing on geomorphic continuity through a riffle-pool sequence. *Geomorphology*, 231, 258–269. Available from: <https://doi.org/10.1016/j.geomorph.2014.12.013>
- Chardon, V., Schmitt, L., Arnaud, F., Piégay, H. & Clutier, A. (2021) Efficiency and sustainability of gravel augmentation to restore large regulated rivers: insights from three experiments on the Rhine River (France/Germany). *Geomorphology*, 380, 107639. Available from: <https://doi.org/10.1016/j.geomorph.2021.107639>
- Church, M. (2006) Bed material transport and the morphology of alluvial river channels. *Annual Review of Earth and Planetary Sciences*, 34(1), 325–354. Available from: <https://doi.org/10.1146/annurev.earth.33.092203.122721>
- Church, M. & Hassan, M.A. (1992) Size and distance of travel of unconstrained clasts on a streambed. *Water Resources Research*, 28(1), 299–303. Available from: <https://doi.org/10.1029/91WR02523>
- Clark, M.J., Bennett, G.L., Ryan-Burkett, S.E., Sear, D.A. & Franco, A.M.A. (2022) Untangling the controls on bedload transport in a wood-loaded river with RFID tracers and linear mixed modelling. *Earth Surface Processes and Landforms*, 47(9), 2283–2298. Available from: <https://doi.org/10.1002/esp.5376>
- Dell'Agnese, A., Brardinoni, F., Toro, M., Mao, L., Engel, M. & Comiti, F. (2015) Bedload transport in a formerly glaciated mountain catchment constrained by particle tracking. *Earth Surface Dynamics*, 3(4), 527–542. Available from: <https://doi.org/10.5194/esurf-3-527-2015>
- Dépret, T. (2014) Fonctionnement morphodynamique actuel et historique des méandres du Cher. Unpublished PhD thesis, Université Paris 1 Panthéon Sorbonne, 530 pp.
- Eaton, B.C. & Church, M. (2011) A rational sediment transport scaling relation based on dimensionless stream power. *Earth Surface Processes and Landforms*, 36(7), 901–910. Available from: <https://doi.org/10.1002/esp.2120>
- Einstein, H.A. (1937) Bedload transport as a probability problem. In: Shen, H.W. (Ed.) *Sedimentation*. Fort Collins: Colorado State University, pp. C1–C105.
- Ergenzinger, P., Schmidt, K.H. & Busskamp, R. (1989) The Pebble Transmitter System (PETS): first results of a technique for studying coarse material erosion, transport and deposition. *Zeitschrift für Geomorphologie*, 33(4), 503–508. Available from: <https://doi.org/10.1127/zfg/33/1989/503>
- Eschbach, D., Grussenmeyer, P., Koehl, M., Guillemin, S. & Schmitt, L. (2021) Combining geodetic and geomorphic methods to monitor restored side channels: feedback from the Upper Rhine. *Geomorphology*, 374, 107372. Available from: <https://doi.org/10.1016/j.geomorph.2020.107372>
- Ferguson, R.I., Bloomer, D.J., Hoey, T.B. & Werritty, A. (2002) Mobility of river tracer pebbles over different timescales. *Water Resources Research*, 38(5), 3-1–3-8. Available from: <https://doi.org/10.1029/2001WR000254>
- Ferguson, R.I., Hoey, T.B., Wathen, S.J., Werritty, A., Hardwick, R.I. & Sambrook Smith, G.H. (1998) Downstream fining of river gravels:

- integrating field, laboratory and modeling study. In: Klingeman, P.C., Beschta, R.L., Komar, P.D. & Bradley, J.B. (Eds.) *Gravel-bed rivers in the environment*. Highlands Ranch, Colorado: Water Resources Publications LLC, pp. 85–114.
- Ferguson, R.I. & Wathen, S.J. (1998) Tracer-pebble movement along a concave river profile: virtual velocity in relation to grain size and shear stress. *Water Resources Research*, 34(8), 2031–2038. Available from: <https://doi.org/10.1029/98WR01283>
- Fields, J., Renshaw, C., Magilligan, F., Dethier, E. & Rossi, R. (2021) A mechanistic understanding of channel evolution following dam removal. *Geomorphology*, 395, 107971. Available from: <https://doi.org/10.1016/j.geomorph.2021.107971>
- Galia, T., Škarpich, V. & Ruman, S. (2021) Impact of check dam series on coarse sediment connectivity. *Geomorphology*, 377, 107595. Available from: <https://doi.org/10.1016/j.geomorph.2021.107595>
- Gilet, L., Gob, F., Gautier, E., Houbrechts, G., Virmoux, C. & Thommeret, N. (2020) Hydro-morphometric parameters controlling travel distance of pebbles and cobbles in three gravel bed streams. *Geomorphology*, 358, 107117. Available from: <https://doi.org/10.1016/j.geomorph.2020.107117>
- Gilet, L., Gob, F., Virmoux, C., Gautier, E., Thommeret, N. & Jacob-Rousseau, N. (2021) Morpho-sedimentary dynamics associated to dam removal. The Pierre Glissotte dam (central France). *Science of the Total Environment*, 784, 147079. Available from: <https://doi.org/10.1016/j.scitotenv.2021.147079>
- Gintz, D., Hassan, M.A. & Schmidt, K.H. (1996) Frequency and magnitude of bedload transport in a mountain river. *Earth Surface Processes and Landforms*, 21(5), 433–445. [https://doi.org/10.1002/\(SICI\)1096-9837\(199605\)21:5%3C433::AID-ESP580%3E3.0.CO;2-P](https://doi.org/10.1002/(SICI)1096-9837(199605)21:5%3C433::AID-ESP580%3E3.0.CO;2-P)
- Gronz, O., Hiller, P.H., Wirtz, S., Becker, K., Iserloh, T., Seeger, M., et al. (2016) Smartstones: a small 9-axis sensor implanted in stones to track their movements. *Catena*, 142, 245–251. Available from: <https://doi.org/10.1016/j.catena.2016.03.030>
- Habersack, H.M. (2001) Radio-tracking gravel particles in a large braided river in New Zealand: a field test of the stochastic theory of bed load transport proposed by Einstein. *Hydrological Processes*, 15(3), 377–391. Available from: <https://doi.org/10.1002/hyp.147>
- Haschenburger, J.K. (1999) A probability model of scour and fill depths in gravel-bed channels. *Water Resources Research*, 35(9), 2857–2869. Available from: <https://doi.org/10.1029/1999WR900153>
- Haschenburger, J.K. (2013) Tracing river gravels: insights into dispersion from a long-term field experiment. *Geomorphology*, 200, 121–131. Available from: <https://doi.org/10.1016/j.geomorph.2013.03.033>
- Haschenburger, J. & Church, M. (1998) Bed material transport estimated from the virtual velocity of sediment. *Earth Surface Processes and Landforms*, 23(9), 791–808. [https://doi.org/10.1002/\(SICI\)1096-9837\(199809\)23:9%3C791::AID-ESP888%3E3.0.CO;2-X](https://doi.org/10.1002/(SICI)1096-9837(199809)23:9%3C791::AID-ESP888%3E3.0.CO;2-X)
- Haschenburger, J.K. & Wilcock, P.R. (2003) Partial transport in natural gravel bed channel. *Water Resources Research*, 39(1), ESG 4-1–ESG 4-9. Available from: <https://doi.org/10.1029/2002WR001532>
- Hassan, M.A. & Bradley, D.N. (2017) Geomorphic controls on tracer particle dispersion in gravel-bed rivers. In: Tsutsumi, D. & Laronne, J.B. (Eds.) *Gravel-bed rivers processes and disasters*. Chichester: John Wiley and Sons, pp. 159–184. <https://doi.org/10.1002/9781118971437.ch6>
- Hassan, M.A. & Church, M. (1992) The movement of individual grains on the streambed. In: Billi, P., Hey, C.R., Thorne, C.R. & Tacconi, P. (Eds.) *Dynamics of gravel-bed rivers*. Chichester: John Wiley and Sons, pp. 159–175.
- Hassan, M.A., Church, M. & Ashworth, P.J. (1992) Virtual rate and mean distance of travel of individual clasts in gravel-bed channels. *Earth Surface Processes and Landforms*, 17(6), 617–627. Available from: <https://doi.org/10.1002/esp.3290170607>
- Hassan, M.A. & Ergenzinger, P. (2003) Use of tracers in fluvial geomorphology. In: Kondolf, G.M. & Piégay, H. (Eds.) *Tools in fluvial geomorphology*. Chichester: John Wiley and Sons, pp. 397–423. <https://doi.org/10.1002/0470868333.ch14>
- Hassan, M.A. & Roy, A.G. (2016) Coarse particle tracing in fluvial geomorphology. In: Kondolf, G.M. & Piégay, H. (Eds.) *Tools in fluvial geomorphology*. Chichester: John Wiley and Sons, pp. 306–323. <https://doi.org/10.1002/9781118648551.ch14>
- Houbrechts, G., Levecq, Y., Peeters, A., Hallot, E., van Campenhout, J., Denis, A.-C., et al. (2015) Evaluation of long-term bedload virtual velocity in gravel-bed rivers (Ardenne, Belgium). *Geomorphology*, 251, 6–19. Available from: <https://doi.org/10.1016/j.geomorph.2015.05.012>
- Houbrechts, G., van Campenhout, J., Levecq, Y., Hallot, E., Peeters, A. & Petit, F. (2012) Comparison of methods for quantifying active layer dynamics and bedload discharge in armoured gravel-bed rivers. *Earth Surface Processes and Landforms*, 37(14), 1501–1517. Available from: <https://doi.org/10.1002/esp.3258>
- Hufnagel, J. & MacVicar, B. (2018) Design and performance of a radio frequency identification scanning system for sediment tracking in a purpose-built experimental channel. *Journal of Hydraulic Engineering*, 144(2), 06017028. Available from: [https://doi.org/10.1061/\(ASCE\)HY.1943-7900.0001412](https://doi.org/10.1061/(ASCE)HY.1943-7900.0001412)
- Imhoff, K.S. & Wilcox, A.C. (2016) Coarse bedload routing and dispersion through tributary confluences. *Earth Surface Dynamics*, 4(3), 591–605. Available from: <https://doi.org/10.5194/esurf-4-591-2016>
- Ivanov, V., Radice, A., Papini, M. & Longoni, L. (2020) Event-scale pebble mobility observed by RFID tracking in a pre-Alpine stream: a field laboratory. *Earth Surface Processes and Landforms*, 45(3), 535–547. Available from: <https://doi.org/10.1002/esp.4752>
- Keller, E.A. & Melhorn, W.N. (1978) Rhythmic spacing and origin of pools and riffles. *Geological Society of America Bulletin*, 89(5), 723–730. [https://doi.org/10.1130/0016-7606\(1978\)89<723:RSAOOP>2.0.CO;2](https://doi.org/10.1130/0016-7606(1978)89<723:RSAOOP>2.0.CO;2)
- Klösch, M. & Habersack, H. (2018) Deriving formulas for an unsteady virtual velocity of bedload tracers. *Earth Surface Processes and Landforms*, 43(7), 1529–1541. Available from: <https://doi.org/10.1002/esp.4326>
- Komar, P.D. & Li, Z. (1986) Pivoting analyses of the selective entrainment of sediments by shape and size with application to gravel threshold. *Sedimentology*, 33(3), 425–436. Available from: <https://doi.org/10.1111/j.1365-3091.1986.tb00546.x>
- Kondolf, G.M. & Matthews, W.V.G. (1986) Transport of tracer gravels on a coastal California river. *Journal of Hydrology*, 85(3–4), 265–280. Available from: [https://doi.org/10.1016/0022-1694\(86\)90060-0](https://doi.org/10.1016/0022-1694(86)90060-0)
- Lamarre, H., mac Vicar, B. & Roy, A.G. (2005) Using passive integrated transponder (PIT) tags to investigate sediment transport in gravel-bed rivers. *Journal of Sedimentary Research*, 75(4), 736–741. Available from: <https://doi.org/10.2110/jsr.2005.059>
- Lamarre, H. & Roy, A.G. (2008a) A field experiment on the development of sedimentary structures in a gravel-bed river. *Earth Surface Processes and Landforms*, 33(7), 1064–1081. Available from: <https://doi.org/10.1002/esp.1602>
- Lamarre, H. & Roy, A.G. (2008b) The role of morphology on the displacement of particles in a step-pool river system. *Geomorphology*, 99(1–4), 270–279. Available from: <https://doi.org/10.1016/j.geomorph.2007.11.005>
- Lauth, T.J. & Papanicolaou, A.N. (2009) Application of radio frequency tracers to individual and group particle displacement within a laboratory. In: Starrett, S. (Ed.) *World environmental and water resources congress 2009: great rivers*. Kansas City, Missouri: ASCE, pp. 2264–2271. [https://doi.org/10.1061/41036\(342\)225](https://doi.org/10.1061/41036(342)225)
- Le Breton, M., Liébault, F., Baillet, L., Charléty, A., Larose, E. & Tedjini, S. (2022) Dense and long-term monitoring of earth surface processes with passive RFID—a review. *Earth-Science Reviews*, 234, 104225. Available from: <https://doi.org/10.1016/j.earscirev.2022.104225>
- Lenzi, M.A. (2004) Displacement and transport of marked pebbles, cobbles and boulders during floods in a steep mountain stream. *Hydrological Processes*, 18(10), 1899–1914. Available from: <https://doi.org/10.1002/hyp.1456>
- Li, Z. & Komar, P.D. (1986) Laboratory measurements of pivoting angles for applications to selective entrainment of gravel in a current. *Sedimentology*, 33(3), 413–423. Available from: <https://doi.org/10.1111/j.1365-3091.1986.tb00545.x>
- Liébault, F., Bellot, H., Chapuis, M., Klotz, S. & Deschâtres, M. (2012) Bedload tracing in a high-sediment-load mountain stream. *Earth Surface Processes and Landforms*, 37(4), 385–399. Available from: <https://doi.org/10.1002/esp.2245>

- Liébault, F. & Laronne, J.B. (2008) Evaluation of bedload yield in gravel-bed rivers using scour chains and painted tracers: the case of the Esconavette Torrent (Southern French Prealps). *Geodinamica Acta*, 21(1-2), 23–34. Available from: <https://doi.org/10.3166/ga.21.23-34>
- Liedermann, M., Tritthart, M. & Habersack, H. (2013) Particle path characteristics at the large gravel-bed river Danube: results from a tracer study and numerical modelling. *Earth Surface Processes and Landforms*, 38(5), 512–522. Available from: <https://doi.org/10.1002/esp.3338>
- Magilligan, F.J., Roberts, M.O., Marti, M. & Renshaw, C.E. (2021) The impact of run-of-river dams on sediment longitudinal connectivity and downstream channel equilibrium. *Geomorphology*, 376, 107568. Available from: <https://doi.org/10.1016/j.geomorph.2020.107568>
- Maniatis, G. (2021) On the use of IMU (inertial measurement unit) sensors in geomorphology. *Earth Surface Processes and Landforms*, 46(11), 2136–2140. Available from: <https://doi.org/10.1002/esp.5197>
- Mao, L., Dell'Agnese, A. & Comiti, F. (2017) Sediment motion and velocity in a glacier-fed stream. *Geomorphology*, 291, 69–79. Available from: <https://doi.org/10.1016/j.geomorph.2016.09.008>
- Mao, L., Picco, L., Lenzi, M.A. & Surian, N. (2017) Bed material transport estimate in large gravel-bed rivers using the virtual velocity approach. *Earth Surface Processes and Landforms*, 42(4), 595–611. Available from: <https://doi.org/10.1002/esp.4000>
- Mao, L., Toro, M., Carrillo, R., Brardinoni, F. & Fraccarollo, L. (2020) Controls over particle motion and resting times of coarse bed load transport in a glacier-fed mountain stream. *Journal of Geophysical Research: Earth Surface*, 125(4), e2019JF005253. Available from: <https://doi.org/10.1029/2019jf005253>
- May, C.L. & Pryor, B.S. (2014) Initial motion and bedload transport distance determined by particle tracking in a large regulated river. *River Research and Applications*, 30(4), 508–520. Available from: <https://doi.org/10.1002/rra.2665>
- McDowell, C., Gaeuman, D. & Hassan, M.A. (2021) Linkages between bedload displacements and topographic change. *Earth Surface Processes and Landforms*, 46(15), 3127–3142. Available from: <https://doi.org/10.1002/esp.5221>
- McDowell, C. & Hassan, M.A. (2020) The influence of channel morphology on bedload path lengths: insights from a survival process model. *Earth Surface Processes and Landforms*, 45(12), 2982–2997. Available from: <https://doi.org/10.1002/esp.4946>
- McEwan, I.K., Habersack, H.M. & Heald, J.G.C. (2001) Discrete particle modelling and active tracers: new techniques for studying sediment transport as a Lagrangian phenomenon. In: Mosley, P. (Ed.) *Gravel-bed rivers*. V. Wellington, New Zealand: New Zealand Hydrological Society, pp. 339–367.
- McNamara, J.P. & Borden, C. (2004) Observations on the movement of coarse gravel using implanted motion-sensing radio transmitters. *Hydrological Processes*, 18(10), 1871–1884. Available from: <https://doi.org/10.1002/hyp.1453>
- McNamara, J.P., Oatley, J.A., Kane, D.L. & Hinzman, L.D. (2008) Case study of a large summer flood on the North Slope of Alaska: bedload transport. *Hydrology Research*, 39(4), 299–308. Available from: <https://doi.org/10.2166/nh.2008.006>
- McQueen, R., Ashmore, P., Millard, T. & Goeller, N. (2021) Bed particle displacements and morphological development in a wandering gravel-bed river. *Water Resources Research*, 57(2), e2020WR027850. Available from: <https://doi.org/10.1029/2020WR027850>
- McVicar, B.J. & Papangelakis, E. (2022) Lost and found: maximizing the information from a series of bedload tracer surveys. *Earth Surface Processes and Landforms*, 47(2), 399–408. Available from: <https://doi.org/10.1002/esp.5255>
- McVicar, B.J., Piégay, H., Henderson, A., Comiti, F., Oberlin, C. & Pecorari, E. (2009) Quantifying the temporal dynamics of wood in large rivers: field trials of wood surveying, dating, tracking, and monitoring techniques. *Earth Surface Processes and Landforms*, 34(15), 2031–2046. Available from: <https://doi.org/10.1002/esp.1888>
- McVicar, B.J. & Roy, A.G. (2011) Sediment mobility in a forced riffle-pool. *Geomorphology*, 125(3), 445–456. Available from: <https://doi.org/10.1016/j.geomorph.2010.10.031>
- Milan, D.J. (2013) Sediment routing hypothesis for pool-riffle maintenance. *Earth Surface Processes and Landforms*, 38(14), 1623–1641. Available from: <https://doi.org/10.1002/esp.3395>
- Misset, C., Recking, A., Legout, C., Bakker, M., Bodereau, N., Borgniet, L., et al. (2020) Combining multi-physical measurements to quantify bedload transport and morphodynamics interactions in an Alpine braiding river reach. *Geomorphology*, 351, 106877. Available from: <https://doi.org/10.1016/j.geomorph.2019.106877>
- Montgomery, D.R. & Buffington, J.M. (1997) Channel-reach morphology in mountain drainage basins. *Geological Society of America Bulletin*, 109(5), 596–611. [https://doi.org/10.1130/0016-7606\(1997\)109%3C0596:CRMIMD%3E2.3.CO;2](https://doi.org/10.1130/0016-7606(1997)109%3C0596:CRMIMD%3E2.3.CO;2)
- Mosley, M.P. (1978) Bed material transport in the Tamaki River near Dannevirke, North Island, New Zealand. *New Zealand Journal of Science*, 21, 619–626.
- Nichols, M.H. (2004) A radio frequency identification system for monitoring coarse sediment particle displacement. *Applied Engineering in Agriculture*, 20(6), 783–787. Available from: <https://doi.org/10.13031/2013.17727>
- Olinde, L. & Johnson, J.P.L. (2015) Using RFID and accelerometer-embedded tracers to measure probabilities of bed load transport, step lengths, and rest times in a mountain stream. *Water Resources Research*, 51(9), 7572–7589. Available from: <https://doi.org/10.1002/2014WR016120>
- Oss Cazzador, D., Rainato, R., Mao, L., Martini, L. & Picco, L. (2021) Coarse sediment transfer and geomorphic changes in an alpine headwater stream. *Geomorphology*, 376, 107569. Available from: <https://doi.org/10.1016/j.geomorph.2020.107569>
- Paola, C., Parker, G., Seal, R., Sinha, S.K., Southard, J.B. & Wilcock, P.R. (1992) Downstream fining by selective deposition in a laboratory flume. *Science*, 258(5089), 1757–1760. Available from: <https://doi.org/10.1126/science.258.5089.1757>
- Paola, C. & Seal, R. (1995) Grain size patchiness as a cause of selective deposition and downstream fining. *Water Resources Research*, 31(5), 1395–1407. Available from: <https://doi.org/10.1029/94WR02975>
- Papangelakis, E. & MacVicar, B. (2020) Process-based assessment of success and failure in a constructed riffle-pool river restoration project. *River Research and Applications*, 36(7), 1222–1241. Available from: <https://doi.org/10.1002/rra.3636>
- Papangelakis, E., McVicar, B. & Ashmore, P. (2019) Bedload sediment transport regimes of semi-alluvial rivers conditioned by urbanization and stormwater management. *Water Resources Research*, 55(12), 10565–10587. Available from: <https://doi.org/10.1029/2019WR025126>
- Papangelakis, E., Muirhead, C., Schneider, A. & McVicar, B. (2019) Synthetic radio frequency identification tracer stones with weighted inner ball for burial depth estimation. *Journal of Hydraulic Engineering*, 145(12), 06019014-1. Available from: [https://doi.org/10.1061/\(ASCE\)HY.1943-7900.0001650](https://doi.org/10.1061/(ASCE)HY.1943-7900.0001650)
- Parker, G. (1991a) Selective sorting and abrasion of river gravel. I: theory. *Journal of Hydraulic Engineering*, 117(2), 131–147. Available from: [https://doi.org/10.1061/\(ASCE\)0733-9429\(1991\)117:2\(131\)](https://doi.org/10.1061/(ASCE)0733-9429(1991)117:2(131))
- Parker, G. (1991b) Selective sorting and abrasion of river gravel. II: applications. *Journal of Hydraulic Engineering*, 117(2), 150–171. Available from: [https://doi.org/10.1061/\(ASCE\)0733-9429\(1991\)117:2\(150\)](https://doi.org/10.1061/(ASCE)0733-9429(1991)117:2(150))
- Parker, G., Klingeman, P.C. & McLean, D.G. (1982) Bedload and size distribution in paved gravel-bed streams. *Proceedings of the American Society of Civil Engineers, Journal of the Hydraulics Division*, ASCE, 108(4), 544–571. Available from: <https://doi.org/10.1061/JYCEAJ.0005854>
- Peeters, A., Houbrechts, G., de le Court, B., Hallot, E., van Campenhout, J. & Petit, F. (2021) Suitability and sustainability of spawning gravel placement in degraded river reaches, Belgium. *Catena*, 201, 105217. Available from: <https://doi.org/10.1016/j.catena.2021.105217>
- Peeters, A., Houbrechts, G., Hallot, E., van Campenhout, J., Gob, F. & Petit, F. (2020) Can coarse bedload pass through weirs? *Geomorphology*, 359, 107131. Available from: <https://doi.org/10.1016/j.geomorph.2020.107131>
- Petit, F., Houbrechts, G., Peeters, A., Hallot, E., van Campenhout, J. & Denis, A.-C. (2015) Dimensionless critical shear stress in gravel-bed

- rivers. *Geomorphology*, 250, 308–320. Available from: <https://doi.org/10.1016/j.geomorph.2015.09.008>
- Phillips, C.B. & Jerolmack, D.J. (2014) Dynamics and mechanics of bedload tracer particles. *Earth Surface Dynamics*, 2(2), 513–530. Available from: <https://doi.org/10.5194/esurf-2-513-2014>
- Phillips, C.B., Martin, R.L. & Jerolmack, D.J. (2013) Impulse framework for unsteady flows reveals superdiffusive bed load transport. *Geophysical Research Letters*, 40(7), 1328–1333. Available from: <https://doi.org/10.1002/grl.50323>
- Piégay, H., Arnaud, F., Cassel, M., Dépret, T., Alber, A., Michel, K., et al. (2016) Suivi par RFID de la mobilité des galets: retour sur 10 ans d'expérience en grandes rivières. *Bulletin de la Société Géographique de Liège*, 67, 77–91.
- Plumb, B.D., Annable, W.K., Thompson, P.J. & Hassan, M.A. (2017) The impact of urbanization on temporal changes in sediment transport in a gravel bed channel in Southern Ontario, Canada. *Water Resources Research*, 53(10), 8443–8458. Available from: <https://doi.org/10.1002/2016WR020288>
- Pretzlav, K.L.G., Johnson, J.P.L. & Bradley, D.N. (2020) Smartrock transport in a mountain stream: bedload hysteresis and changing thresholds of motion. *Water Resources Research*, 56(11), e2020WR028150. Available from: <https://doi.org/10.1029/2020WR028150>
- Pretzlav, K.L.G., Johnson, J.P.L. & Bradley, D.N. (2021) Smartrock transport from seconds to seasons: shear stress controls on gravel diffusion inferred from bed and rest scaling. *Geophysical Research Letters*, 48(9), e2020GL091991. Available from: <https://doi.org/10.1029/2020GL091991>
- Rainato, R., Mao, L. & Picco, L. (2018) Near-bankfull floods in an Alpine stream: effects on the sediment mobility and bedload magnitude. *International Journal of Sediment Research*, 33(1), 27–34. Available from: <https://doi.org/10.1016/j.ijsrc.2017.03.006>
- Rainato, R., Mao, L. & Picco, L. (2020) The effects of low-magnitude flow conditions on bedload mobility in a steep mountain stream. *Geomorphology*, 367, 107345. Available from: <https://doi.org/10.1016/j.geomorph.2020.107345>
- Roberts, M.O., Renshaw, C.E., Magilligan, F.J. & Brian, D.W. (2020) Field measurement of the probability of coarse-grained sediment entrainment in natural rivers. *Journal of Hydraulic Engineering*, 146(4), 04020024-1. Available from: [https://doi.org/10.1061/\(ASCE\)HY.1943-7900.0001694](https://doi.org/10.1061/(ASCE)HY.1943-7900.0001694)
- Rollet, A.J. (2007) *Etude et gestion de la dynamique sédimentaire d'un tronçon fluvial à l'aval d'un barrage: le cas de la basse vallée de l'Ain*. Unpublished PhD thesis. Université Jean Moulin Lyon 3, 306 pp.
- Rollet, A.J., MacVicar, B., Piégay, H. & Roy, A. (2008) L'utilisation de transpondeurs passifs pour l'estimation du transport sédimentaire: premiers retours d'expérience. *La Houille Blanche*, 4, 110–116.
- Schick, A.P., Lekach, J. & Hassan, M.A. (1987) Bed load transport in desert floods: observations in the Negev. In: Thorne, C.R., Bathurst, J.C. & Hey, R.D. (Eds.) *Sediment transport in gravel-bed rivers*. Chichester: John Wiley and Sons, pp. 617–642.
- Schmidt, K.H. & Ergenzinger, P. (1992) Bedload entrainment, travel lengths, step lengths, rest periods studied with passive (iron, magnetic) and active (radio) tracer techniques. *Earth Surface Processes and Landforms*, 17(2), 147–165. Available from: <https://doi.org/10.1002/esp.3290170204>
- Schmidt, K.H. & Gintz, D. (1995) Results of bedload tracer experiments in a mountain river. In: Hickin, E.J. (Ed.) *River geomorphology*. Chichester: John Wiley and Sons, pp. 37–54.
- Schneider, J., Hegglin, R., Meier, S., Turowski, J.M., Nitsche, M. & Rickenmann, D. (2010) Studying sediment transport in mountain rivers by mobile and stationary RFID antennas. In: Dittrich, K., Koll, A., Aberle, J. & Geisenhainer, P. (Eds.) *5th international conference on fluvial hydraulics (river flow 2010)*. Braunschweig, Germany: Bundesanstalt für Wasserbau, pp. 1723–1730.
- Schneider, J.M., Turowski, J.M., Rickenmann, D., Hegglin, R., Arrigo, S., Mao, L., et al. (2014) Scaling relationships between bed load volumes, transport distances, and stream power in steep mountain channels. *Journal of Geophysical Research: Earth Surface*, 119(3), 533–549. Available from: <https://doi.org/10.1002/2013JF002874>
- Sear, D.A. (1996) Sediment transport processes in pool-riffle sequences. *Earth Surface Processes and Landforms*, 21(3), 241–262. [https://doi.org/10.1002/\(SICI\)1096-9837\(199603\)21:3<241::AID-ESP623>3.0.CO;2-1](https://doi.org/10.1002/(SICI)1096-9837(199603)21:3<241::AID-ESP623>3.0.CO;2-1)
- Stähly, S., Franca, M.J., Robinson, C.T. & Schleiss, A.J. (2020) Erosion, transport and deposition of a sediment replenishment under flood conditions. *Earth Surface Processes and Landforms*, 45(13), 3354–3367. Available from: <https://doi.org/10.1002/esp.4970>
- Sternberg, H. (1875) Untersuchungen über Längen und Querprofil geschiefte Flüsse. *Z. Bauwesen*, 25, 483–506.
- Tsakiris, A., Papanicolaou, A., Moustakidis, I. & Abban, B. (2015) Identification of the burial depth of radio frequency identification transponders in riverine applications. *Journal of Hydraulic Engineering*, 141(6), 04015007. Available from: [https://doi.org/10.1061/\(ASCE\)HY.1943-7900.0001001](https://doi.org/10.1061/(ASCE)HY.1943-7900.0001001)
- Vázquez-Tarrió, D., Arnaud, F., Cassel, M., Dépret, T., Meric, L., Michel, K., et al. (2021) *Suivi de l'effet morphologique du démantèlement des marges : validation des estimations de charriage par des observations in situ*. Unpublished technical report. Observatoire des Sédiments du Rhône, 58 pp.
- Vázquez-Tarrió, D., Piqué, G., Vericat, D. & Batalla, R.J. (2021) The active layer in gravel-bed rivers: an empirical appraisal. *Earth Surface Processes and Landforms*, 46(2), 323–343. Available from: <https://doi.org/10.1002/esp.5027>
- Vázquez-Tarrió, D., Recking, A., Liébault, F., Tal, M. & Menéndez-Duarte, R. (2019) Particle transport in gravel-bed rivers: revisiting passive tracer data. *Earth Surface Processes and Landforms*, 44(1), 112–128. Available from: <https://doi.org/10.1002/esp.4484>
- Wilcock, P.R. & McArdeil, B.W. (1993) Surface-based fractional transport rates: mobilization thresholds and partial transport of a sand-gravel sediment. *Water Resources Research*, 29(4), 1297–1312. Available from: <https://doi.org/10.1029/92WR02748>

SUPPORTING INFORMATION

Additional supporting information can be found online in the Supporting Information section at the end of this article.

How to cite this article: Liébault, F., Piégay, H., Cassel, M. & Arnaud, F. (2023) Bedload tracing with RFID tags in gravel-bed rivers: Review and meta-analysis after 20 years of field and laboratory experiments. *Earth Surface Processes and Landforms*, 1–23. Available from: <https://doi.org/10.1002/esp.5704>